On The Mechanistic Basis of Deformation at the Microscale in Hexagonal Close Packed Metals

T.B. Britton[a1], F.P.E. Dunne[a2], A.J. Wilkinson[b3]

a. Department of Materials, Imperial College London, Prince Consort Road, London, SW7 2AZ

b. Department of Materials, University of Oxford, Parks Road, Oxford, OX1 3PH

1. b.britton@imperial.ac.uk

2. fionn.dunne@imperial.ac.uk

3. angus.wilkinson@materials.ox.ac.uk

Keywords: deformation, metals, mechanics, alloy

1. Abstract

This is an overview of micromechanical deformation mechanisms in hexagonal close packed (HCP) metals. We start with an in-depth discussion of single crystal behaviour concerning crystallographic slip, plastic anisotropy and deformation twinning. We move on to discuss some complexities involved in polycrystalline deformation, modelling approaches and focus on rate effects in titanium alloys that are thought to play a significant rôle in dwell fatigue. We finish our review with a brief commentary on current understanding, state-of-the-art techniques and outline some key areas where further study is recommended.

2. Glossary

AFM – atomic force microscopy

BOR - Burger orientation relationship

BCC – body centred cubic

CRSS – critical resolved shear stress

EBSD – electron backscatter diffraction

EPSC – elasto-plastic self-consistent

EVPSC – elasto-viscoplastic self-consistent

FEA – finite element analysis

FIB – focussed ion beam

GB – grain boundary

GND – geometrically necessary dislocation

FFT – fast Fourier transform

HCP – hexagonal close packed

PTS - predominant twin system

SRO – short range order

TEM – transmission electron microscopy

3. Introduction

Hexagonal close packed (HCP) metals[1] are used in a wide variety of engineering sectors, including aerospace, nuclear, automotive, scientific instrumentation, chemical engineering, and bio-engineering. The metals and alloys are used due to the combination of excellent mechanical properties, corrosion resistance and the ability to engineer new chemistries and thermo-mechanical treatments to tailor their microstructure, and hence properties, for a particular application.

The engineering use of HCP metals is widespread, for example: titanium is used in fan blades in jet engines, corrosion resistance piping and biomedical implants; zirconium is used in fuel cladding in nuclear fission reactors; magnesium is used in automotive applications such as steering wheels and intake manifolds; zinc is used as coating for steels; and beryllium is used in scientific instrumentation and nuclear fusion reactors. The other HCP metals (cobalt, cadmium, rhenium, hafnium and ruthenium) are used less extensively.

The HCP unit cell imparts significant anisotropy on their mechanical performance at the microscale (as well as other properties) which often leads to more difficult processing routes and requires careful exploitation in high performance applications. To drive further applications of this important class of materials it is timely to review fundamental deformation mechanisms at the microstructure length scales, i.e. micromechanical deformation mechanisms, to identify state-of-the-art advances as well as opportunities for further study.

This review describes mechanistic studies and insight into the deformation of HCP alloys starting with single crystal slip with a discussion on the fundamentals of slip and alloying. This continues with a brief discussion on twinning focusing down on three of the metals – Zr, Ti and Mg – used in high value engineering applications. To demonstrate industrial relevance and promote appreciation of these fundamental concepts, we provide this together with an in-depth discussion of methods and approaches to study polycrystalline deformation in Ti alloys for aerospace applications. We conclude with a brief summary of current and future opportunities to enable this important and transformative class of materials to deliver the next generation of engineering components.

4. Single crystal anisotropy

4.1 The Slip Systems

Hexagonal symmetry leads to considerable anisotropy in the elastic and plastic mechanical properties of HCP metals, as well as other physical properties. The slip systems, illustrated in List of figures:

[1] We note that HCP metals are not strictly closed packed, according to the ideal rigid ball model, see Table 1, but we stick with the term ‘Hexagonal Close Packed’ or HCP as per convention within this field.

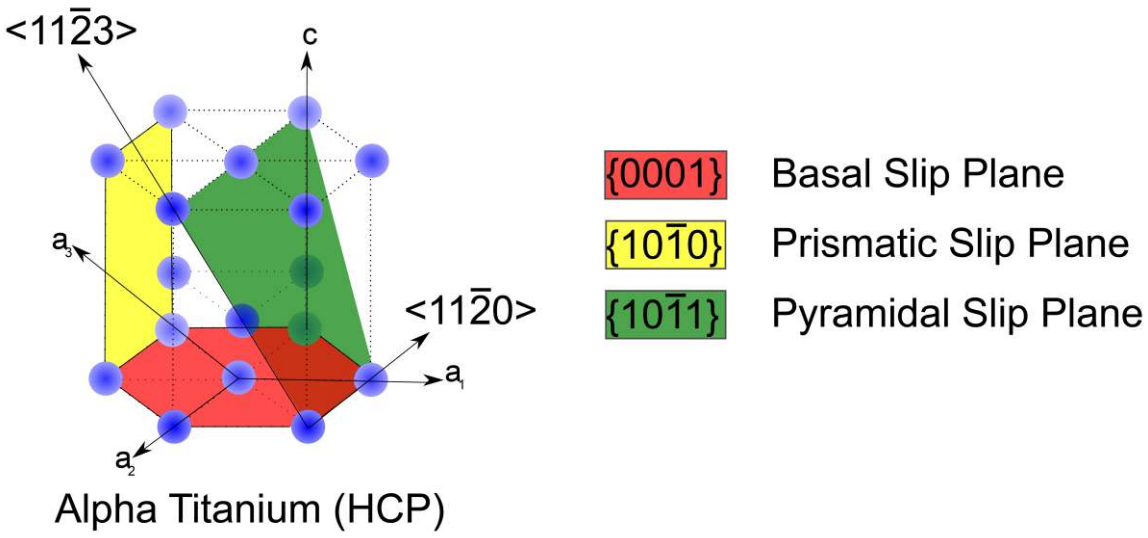

Figure 1, have been identified as playing a significant rôle in the plastic deformation of HCP metals and alloys.

The $\frac{a}{3}$<11$\bar{2}$0> or <a> directions are the close packed directions and are thus the shortest Burgers vector possible for perfect dislocations. <a> type dislocations have been shown to slip on several different slip planes including (0001) basal, $\{10\bar{1}0\}$ prismatic, and $\{10\bar{1}1\}$ pyramidal. The three <a> Burgers vectors are co-planar within the basal plane and so only offer two independent slip directions. To fully support an arbitrary plastic strain, and so satisfy the von Mises deformation criterion, modes that generate shear displacement out of the basal plane are required. Dislocations with $\frac{a}{3}$<11$\bar{2}$3> or <c+a> Burgers vectors have been found in many HCP metals and these along with deformation twinning (see section 4) provide the additional deformation modes. The <c+a> dislocations have Burgers vectors that are significantly longer than for the <a> dislocations and hence are energetically less favoured and tend to have higher resistance to motion.

4.2 Determining Critical Resolved Shear Stresses

The most direct way to establish the critical resolved shear stress (CRSS), which is the preferred measure of resistance to slip on a given slip system, is to conduct a macroscopic tension or compression test on a suitably oriented single crystal sample. A considerable body of work of this type has been undertaken, predominately in the 1950s, 60s and 70s, to establish the fundamentals of CRSS values for the important slip systems in the pure HCP metals (eg [1-4]). Growth of the single crystals is itself a major undertaking, especially where a solid state allotropic phase transformation occurs (eg in Zr and Ti). The orientation of the crystal is typically determined using laboratory based Laue X-ray diffraction in the reflection geometry. The crystal can then be cut at a suitable orientation so that loading causes a large resolved shear stress on the selected target slip system while minimising the stress on others. These high purity single crystals are typically very soft and have to be treated carefully. Growth of large single crystals of the more highly alloyed systems has often proved prohibitively difficult and now that data for the pure metals and lightly alloyed systems has been established the approach has seen limited subsequent application.

An alternative approach makes use of in situ deformation of a polycrystalline sample while recording X-ray or neutron diffraction patterns along with appropriate crystal plasticity simulations. The CRSSs of the various slip systems are adjusted in the model using an iterative scheme so that a good fit is obtained to the bulk stress-strain response, and to the lattice strain evolution for various grain orientation families probed by the diffraction experiment. The 'grain families' consist of all the grains within the diffraction volume that contribute to a given diffraction peak and so average over a range of possible grain orientations that are dispersed through the material in grains with differing nearest neighbour environments. The simulations are seeded with grain orientations that represent the macroscopically measured texture. Turner and Tome [5] appear to have been the first to take such an approach using an elasto-plastic self-consistent (EPSC) model to extract CRSS values for slip modes in Zircaloy-2 from neutron diffraction measurements of residual stresses. Previous related work by Lebensohn and Tome [6] used a viscoplastic formulation along with texture development to imply yield and hardening behaviour over much larger strains again in Zircaloy materials. These early works used models in which grains are considered as ellipsoidal inclusions in a homogenised matrix which are analysed using a framework developed by Eshelby [7, 8]. The scheme is iterated so that the average behaviour of the individual grain inclusion is consistent with the properties of the *homogenised equivalent matrix*. The EPSC approach is computationally very efficient but the effects of the individual grain environments are 'smeared out' and stress variations within the grains are removed through use of the Eshelby ellipsoidal inclusion result. This problem is exacerbated in low symmetry materials such as the HCP metals, as local neighbour effects can be quite strong. As computing power has increased, the EPSC model has tended to be replaced with a crystal plasticity finite element analysis (FEA) simulation, or most recently with fast Fourier transform (FFT) image-based simulations [9-11]. These more modern approaches remove some of the short comings of the EPSC model by allowing intragranular stress variations and grain-grain interactions. However the approach relies on simultaneously fitting multiple model parameters to multi-variable experimental datasets. Errors in the best fit materials parameters are difficult to assess as they combine both limitations of the model assumed and uncertainties in the experimental measurements which are linked in complex ways.

A further class of methods to obtain CRSS values are based on deforming small volumes of material within individual grains of a polycrystal. Merson et al [12] and Viswanathan et al [13] noted the marked change in hardness when performing nanoindentation into selected grains within Ti alloys with surface normal parallel (harder and more stiff) or perpendicular (softer and less stiff) to the basal plane. Here the difficulty lies in extracting the exact slip systems that are operating in the very complex loading environment surrounding the indenter tip. A more detailed investigation by Britton et al [14] linked nanoindentation data to high resolution electron backscatter diffraction (EBSD) measurements of the lattice curvature and residual stresses, and atomic force microscopy (AFM) measurements of the surface topography to better understand the flow fields near indents in differently oriented grains. They also conducted crystal plasticity FEA simulations using a strain gradient plasticity formulation with CRSS values adjusted to give a good fit to the experimental load-displacement data for differently oriented grains, and made comparison with topography, lattice rotation and strain fields obtained experimentally. Zambaldi et al [15] have also used crystal plasticity modelling, orientation measurements with EBSD and AFM to study deformation around conical indents in commercially pure Ti; however, the omission of any size effects in their simulations means that the CRSS values extracted may be a little high. Furthermore a lack of

measurements with loading along the <c> axis may result in increased uncertainty on the CRSS for the <c+a> type slip system. Although the nanoindentation clearly demonstrates anisotropy in hardness and crystallographic effects on the flow fields, extraction of reliable quantitative CRSS values is difficult due to the complex stress and strain fields during indentation which leads to multiple slip and hardening from slip system interactions, as well as the indentation size effect from the imposed strain gradients.

In order to isolate the plastic response into a single targeted slip system it is possible to use a focused ion beam (FIB) to machine micron-scaled test pieces (compression pillars or bend beams) from individual polycrystals of particular crystallographic orientation that can then be tested in a nano-indenter or other bespoke small scale testing apparatus. This greatly simplifies the task of interpreting the load-displacement data compared to nanoindentation and only a single CRSS value need be extracted from a given test. The major issues with testing such small volumes are the 'smaller is stronger' size effects and the stochastic nature of the plastic flow [16].

In the bending geometry the strain gradients and retention of dislocations in the low stress regions near the neutral axis tends to reduce the relative size of the strain bursts or load drops seen compared to the compression case. There also seems to be good agreement on the nature and cause of the size effect seen in micro-cantilever testing allowing extrapolation to bulk values to be made with more confidence. Gong and co-workers [17-20] have made extensive use of micro-cantilevers to study CRSS values for the major slip systems in various Ti alloys. This has included work with Ding et al using FIB on deformed micro-cantilevers to make thin foils for post-mortem transmission electron microscopy (TEM) analysis of the dislocation structures obtained [21, 22]. The bending geometry requires that crystal plasticity FEA simulations are used to obtain the CRSS values through a procedure using forward modelling and comparison to experiment. Recent work by Tarelton et al. [23] have linked these types of experimental single crystal measurements of micro-cantilever bending with a planar 2D discrete dislocation dynamics model and demonstrated that there may be a strong size dependence inherited not only from soft pile ups in the zero stress region, but also due to the density of sources in these limited volumes.

Micro-pillar compression has been used for measurements on Mg alloys in basal slip and twinning [24-27] and in Ti alloys for prismatic slip and twining [28, 29]. Generally no FEA modelling is undertaken and load and displacement are simply converted to engineering stress and strain from measurements of the pillar cross-section and height, although the strains are typically overestimated due to deformation below the pillar which effectively acts as a blunt punch. A common shortcoming in interpretation of much of the micro-pillar compression data has been an insistence on using a simple power law scaling for analysing the length scale effects; this is unphysical as extrapolation to the bulk leads to zero strength. This has been emphasised by Dunstan and Bushby [30] who have reanalysed micro-pillar compression data to include finite bulk strength.

Metal	c/a ratio	preferred slip system	purity	<a> Basal CRSS (MPa)	<a> Prism CRSS (MPa)	Reference
Cd	1.886	<a> basal	99.996	0.2		Roscoe 1936 [31]
Zn	1.856	<a> basal	99.999	0.2		Jillson 1950 [32]
Ideal	1.633	Hard sphere model				
Mg	1.624	<a> basal	99.996	0.8		Burke & Hibbard 1952 [33]
Co	1.623	<a> basal				
Re	1.615	<a> basal		9.0	16.5	Jeffery & Smith 1960 [34]
Zr	1.593	<a> prism	99.98	>24	6.4	Rapperport 1959 [35]
Ti	1.588	<a> prism	99.95	92	23.5	Levine 1966 [36]
Ru	1.582	<a> prism	99.92		20.6	Snow & Breedis 1974 [37]
Hf	1.581	<a> prism	98.6		20	Das & Mitchell 1973 [38]
Be	1.568	<a> basal	99.	2.3	14.7	Turner & White 1972 [39]

Table 1: c/a ratio, preferred slip system and critical resolved shear stresses of pure HCP metals.

4.3 Critical Resolved Shear Stresses for Pure Metals

<a> dislocations are the dominant dislocation types and the naive expectation of near exclusive slip on the close packed plane is to some extent borne out [2] as table 1 shows that basal slip tends to be preferred when the c/a ratio is close to the ideal value obtained for close packing of hard spheres. However, the relative ease of slip on the <a> basal slip system decreases as the c/a ratio decreases (Table 1). A distinct anomaly in this is Be which has a particularly low c/a ratio but still exhibits <a> basal slip as its easiest slip system. Bacon & Vitek [40] point out that d-electrons may play a significant rôle in promoting <a> prism slip over basal slip. The dislocation core structures cannot be predicted unless simulations correctly capture the interatomic bonding and in particular the directional covalent-like nature to which d-orbitals contribute significantly. Calculations for <a> screw dislocations in Ti showed two low energy configurations with the core either splitting into two distinct Shockley partials on the basal plane, or spreading more continuously on the prism plane. Finnis–Sinclair-type potentials do not fully capture the directional effects and tend to under-predict the basal plane stacking fault energy, and thus wrongly predict basal plane splitting as the lower energy configuration. However, when the more realistic bond-order-potentials are used, which better represent d-electron effects on directional bonding, higher basal stacking fault energies are predicted and the preferred low energy configuration is correctly identified, with the core spreading on the prism plane [41]. More recent density functional theory (DFT) calculations for Ti have confirmed the lower energy core configurations involve disassociation on the prism plane [42, 43]. Like Ti the metals Zr and Hf are also group 4 d-block elements and prism slip occurs more readily for similar reasons. The absence of any d-electrons in Be may result in a lower basal plane stacking fault energy and stabilize dissociation into Shockley partials on the basal plane. Adhikari and Mukhopadhyay [44] suggest that bonding within the basal plane of Be is metallic but along the <c> axis tends to have a more covalent character.

Deformation temperature and strain rate have significant effects on CRSS values. Strain rate and temperature jump tests have been used to extract CRSS data from single crystals over a wider range of conditions and to allow activation volumes to be probed in addition to activation energies [45]. Figure 2 shows CRSS values as a function of temperature for pure Ti [2, 36, 46-48], Zr [1, 3, 4, 45] and Mg [49] at very low interstitial impurity levels. Basal slip in Mg has a markedly lower CRSS value than either prism or basal slip in Ti and Zr as shown in figure 2. The behaviour of Ti and Zr is very similar

with CRSS values for <a> prism slip being radically lower than for <a> basal at low temperatures but becoming more similar at high temperatures. The activation energy for <a> basal slip is larger than for <a> prism slip in these two metals. At high purities ([Oeq] < 0.2at%, see Eq 1) there are anomalous peaks in both the activation energies and activation volumes reported for both basal and prism slip close to room temperature [50]. However at higher interstitial contents, typical of commercial materials, this anomalous behaviour is supressed [50]. Thermal activation, particularly in relation to the near room-temperature creep behaviour is of particular technological interest as discussed in section 6. There is a clear need for further research to understand the atomistic mechanisms controlling the slip rate sensitivity of the different slip systems and how they are influenced by alloying.

At low strains (stage I) prism slip is associated with a well-separated planar slip lines on the sample surface. As stage II is reached other secondary slip features can be observed. Diffraction contrast in the TEM reveals long dislocation lines predominately of screw character aligned along the <$11\bar{2}0$> directions, with densities of 10^{12} - 10^{13} m^{-2} typical for deformation of a few per cent strain [50]. Surface slip lines observed for basal slip orientations, with screw orientations tending to be aligned with <$11\bar{2}0$>, have been reported in both Ti and Zr as more wavy in nature and associated with cross-slip onto the prism plane for which dissociation into partials is more favoured [1, 2].

<a> slip on prism and basal planes is not sufficient to satisfy the von Mises criterion and thus accommodate an arbitrary plastic strain. For example tension or compression along the c-axis cannot be achieved without slip of dislocations with Burgers vectors along <c+a> or $\frac{1}{3}\langle 11\bar{2}3\rangle$ or twinning (see section 5). <c+a> slip has been shown to be a significant deformation mode in many HCP metals including Ti [51] and Zr [52]. The CRSS values for <c+a> slip are considerably larger than for the <a> slip systems and comparable to those for twinning so that both modes are often activated which complicates interpretation of mechanical test data. Williams et al [53] showed that alloying with Al increases the CRSS for <c+a> slip but inhibits twinning more.

The use of CRSS and dislocation activity can be used to inform discrete dislocation dynamics (DDD) models in 2D and 3D and these models can be used to understand mechanisms involved in hardening and micro-plasticity involving the interactions of multiple dislocations in real structures. Monnet et al. [54] constructed a 3D DDD model of Zr, involving both crystal slip and thermally activated processes, to understand limited forest hardening at low temperatures due to the continuous multiplication of screw dislocations of a well oriented single slip system. Observations of this type can be used to inform models at longer length scales (see Section 6 and for example reference [55]).

4.4 Effects of Alloying

The small atomic radii of oxygen, nitrogen and carbon atoms allow them to adopt octahedral interstitial sites in the HCP metals [56] and these have very pronounced effects even at low concentrations on the CRSS values. The oxygen equivalent content can be used to group strengthening contributions from oxygen, nitrogen and carbon according to their potency [57]:

$[O_{eq}] = [O] + 2.0\,[N] + 0.75\,[C]$, where [X] is the at% of element X. Eq 1

Figure 3 shows CRSS values obtained by different authors for basal and prism slip at room temperature in Ti and prism slip in Zr over a range of oxygen equivalent concentrations. Although increased oxygen content increases the strength of both prism and basal slip in Ti the effect is much more marked for the easier prism slip. Very recent work by Yu et al [58] has shown through advanced STEM imaging and DFT calculation that although the core of edge dislocations in Ti was relatively unaffected by increasing the oxygen content from 0.1wt% to 0.3wt% (~0.3 to 0.9at%), the cores of screw dislocations were profoundly altered narrowing significantly as the oxygen content increased. DFT suggests very intense localised repulsion between a screw dislocation and interstitial oxygen on octahedral sites on the same prismatic plane as the dislocation which may promote cross-slip close to the oxygen to remove the dislocation from this energetically undesirable site and generating edge segments that are unable to glide on the prismatic plane. For commercial Ti alloys the lowest interstitial content is for ASTM grade 1 which has a maximum allowable oxygen equivalent of a little over 1at% (summing contributions from oxygen, nitrogen and carbon); this increases through grades 2 and 3 to grade 4 which can have an oxygen equivalent of up to 1.8at%. At these higher interstitial levels there is relatively little difference between the CRSS values for prism and basal slip in Ti, though of course prism slip offers more slip planes and so predominates in deformation of polycrystals. At increased oxygen levels there is also a change in slip mode from wavy to planar slip at lower temperatures due to increased difficulty of cross-slip [59, 60].

Figure 3 also includes data from Zr and Zircaloy-2 recorded at room temperature, where deformation is restricted to prism slip as deformation twinning tends to complicate extraction of CRSS values for purely basal slip. Interstitials in Zr are seen to have a similar effectiveness in hardening prism slip systems. Zr alloy systems tend to be less highly alloyed than Ti systems and the oxygen interstitial content typical in commercial alloys (in the range 0.10 to 0.14 wt%, or ~0.6 to 0.8at%) makes a significant contribution to strength at room temperature as indicated by inclusion of data for zircaloy-2 in Figure 3.

Interstitial strengthening is coupled with a loss of ductility. This is particularly marked at higher concentrations, where it is linked to a change to planar slip. This can be problematic because exposure of Ti to elevated temperatures in oxygen-containing environments not only causes formation of a surface oxide but also to a much deeper penetrating profile of raised oxygen concentration (‘α-case’). Rugg et al [63] have used orientation-corrected nanoindentation within the surface layer showing significant changes in hardness, as well as micro-cantilevers cut within selected grains oriented for prism slip to show that the CRSS in Ti-6Al-4V approximately doubles across the ~100 μm wide diffusion layer, where atom probe analysis shows the oxygen content increases from 0.4wt% to >1wt%. In components, the α-case layer can lead to a significant drop in performance due to easy crack initiation in either tensile or cyclic loading conditions [64, 65].

Of the substitutional alloying additions to Ti, Al is by far the most common and important. There have been two significant single crystal testing campaigns by Sakai and Fine [66-68] and later by Williams et al [53].

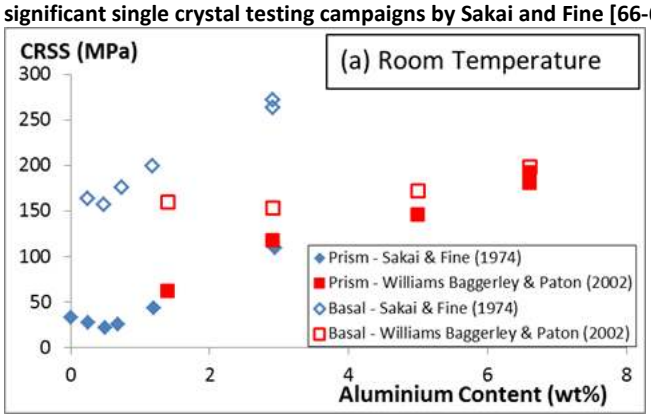

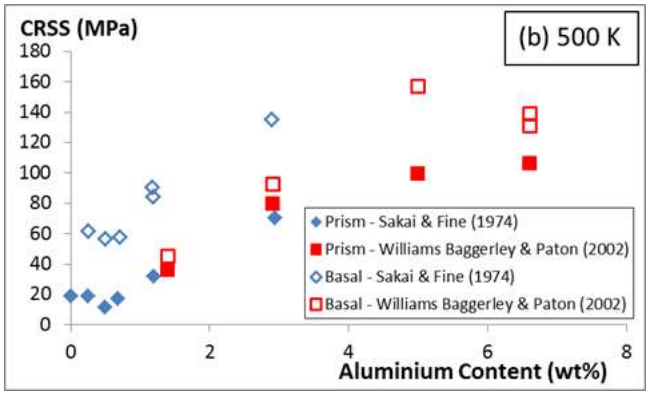

Figure 4 summarises the CRSS data obtained for prism and basal slip in Ti-Al alloys at room temperature and 500 K. There is good agreement between the two studies for prism slip, though for basal slip the shear tests of Sakai and Fine show marked hardening between 0.5wt% and 3wt% while data from the more conventional compression testing of Williams et al indicates relatively little change. Sakai and Fine adopted the shear testing mode because compression testing resulted in twinning and/or prism slip and Williams et al also report that deformation twinning and prism slip were seen in samples compressed with the aim of activating basal slip. Both sets of data do however indicate that increasing Al content and particularly temperature tend to reduce the ratio of CRSS values for basal and prism slip. For prism slip considerable hardening is brought about by Al additions and this is linked to a narrowing of the slip bands with deformation becoming more localised and planar as cross slip is made more difficult. More obviously the basal slip which is relatively wavy in pure Ti becomes planar as Al is added. For their highest Al content (6.6wt%) Williams et al showed prolonged aging could generate a fine dispersion of coherent Ti_3Al α_2 which were destroyed by the passage of dislocations within a slip band. Under less extreme heat treatments and at lower overall Al concentrations clustering and short range order (SRO) in the Al distribution is thought to occur and be responsible for the hardening and increasing slip planarity. Neeraj and Mills [69, 70] have also observed strong effects of SRO on the room temperature creep response of Ti-Al alloys. They altered the cooling profile following a hold at an α-phase homogenisation temperature of 900°C (1173 K), using a rapid quench to supress ordering and slow cooling or a step aging treatment to promote it. Creep rates were markedly lower when SRO was present and the dislocations arrangements demonstrated a very obvious transition to planar slip as SRO was enhanced.

5. Twinning

Easy <a> slip in HCP materials does not provide the necessary five degrees of freedom required for an arbitrary shape change. In some materials, deformation may be accommodated through <c+a> slip, but alternatively twin systems can operate. Twinning enables significant deformation of the lattice through crystal shear, often involving local atomic shuffling [71], with associated lattice reorientation.

In the HCP materials, there are a number of twinning modes which can accommodate deformation; broadly these can be split into the contraction/compression, and the extension/tension twins. The specific language here describes the sense of strain generated by the operation of the twin system along the <c> axis of the parent crystal as each twin system only results in shear in one direction. This can cause some confusion with respect to the applied stress state because tension twins are often found in specific microstructural areas of a compression test where a local crystal has the c-axis orientated perpendicular to the compression axis, and extension is therefore kinematically required.

Typical shears and reorientations associated with twinning in Zr are shown in Figure 5. As the c/a ratio changes so does the associated reorientation and twinning shear (see Figure 6); eg as Yoo [72] notes that this changes for the $\{10\bar{1}2\} < \bar{1}011 >$ system from an extension twin for low c/a materials (Ti, Zr, Be, Re, Mg) to a contraction twin for high c/a materials (Zn, Cd).

In addition to these geometric shear and reorientation relationships, the nature of the HCP lattice often requires additional shuffle steps to accommodate the twinning shear at the atomic scale [71]. A shuffle involves local atomic rearrangement and may dominate the selection of the daughter twin variant and therefore the active twinning mode. For a more complete description of the precise atomic shuffles involved in HCP twins the reader is directed to the review by Christian and Mahajan [71].

Direct observation of the twinning process is difficult due to the rate at which twins form. Therefore studies have either focused on direct modelling of the twin process, using tools such as molecular dynamics, observations of post-twin structures in polycrystals, or crystal plasticity modelling of texture, residual stress or polycrystal microstructures.

Twinning is an important deformation mode, as during processing it can dominate the formation of crystallographic texture. For example, different c/a ratios and active twin systems result in different macroscopic textures, as shown in Figure 7 [73]. In Mg alloys the lack of easy <c+a> slip and predominance of twinning modes results in difficulties in forming Mg components, as very strong textures can be generated with significant anisotropy of mechanical properties which limits their engineering use and available processing routes [74].

5.1 Twinning mechanistic overview

The precise mechanisms of twinning are less well understood than for crystallographic slip. It is thought that twinning can be broken into the following steps: *incubation, nucleation, propagation* and *growth.* Incubation describes the process of accumulation of enough stress within the material to generate a twin nucleus, often through stresses of piled-up dislocations resulting in slip

stimulated mechanisms [75-78] and provides a heterogenous twin nucleation mechanism that requires significantly less stress than the homogenous route found in nearly perfect single crystals [71]. Once sufficient stress is present on the active twinning system, the twin may nucleate through the generation of one, or several, twinning dislocations that contain not only the traditional slip-like Burgers vector, but also a twinning step. Twinning dislocations which have non-rational indices are thought to require a shuffle step to accommodate their movement (i.e. a lattice translation as associated with dislocation slip and an additional lattice step). These are caused by varying interplanar spacings and waviness of the non-basal plane. The CRSS of twinning is dependent not only on the line tension of the initial dislocation, but also is dependent on the surface tension of the twin interfaces [73]. Once the twin nucleus is formed, it may then propagate very rapidly (close to the speed of sound) along the shear displacement direction through the grain causing significant shear as it progresses. After propagation, the twin may then grow perpendicular to the twin plane, or fatten, to form a lenticular ellipsoid [79]. Twin growth can be markedly slower than initial propagation.

The nature of twinning is difficult to understand experimentally, due to the complex interplay of very fine microstructure features, high stresses, and very fast processes. Simulation offers significant insights into potential mechanisms, both at the atomic scale and leading up to the consequences of twinning on texture, microstructure and performance. For example, the work of Wang and colleagues using atomistic simulations has outlined the complex interplay of atomic shuffling, twinning dislocations and local zonal deformation mechanisms which are involved in the initiation and propagation of twins at the atomic scale [80-82].

5.1 Twinning deformation studies

Initial work modelling deformation twinning processes used self-consistent approaches, where twinning is included as a pseudo-slip mode, often called a predominant twin reorientation (PTR) scheme, which only allows deformation in one direction. Agnew et al. [83] performed multi-axial deformation, including in-plane compression of the Mg alloy AZ31B with basal texture which showed lots of twinning with complete reorientation of the texture. Neutron diffraction measurement of internal strains was combined with self-consistent modelling using a Voce hardening law with initial CRSS and final (back extrapolated) CRSS from the model. They considered the following deformation modes: <a> on prism, <a> on basal, <c+a> on second order pyramidal, and tensile deformation twinning on $\{10\bar{1}2\}$ planes. As this sample and total strain shows minimal texture evolution, the self-consistent model could be used to extract the following: $\{10\bar{1}2\}$ extension twinning to have a τ_0 of 30MPa; basal <a> τ_{crss} 10MPa and prism <a> τ_{crss} of 55MPa, and <c+a> τ_{crss} of 60MPa, with hardening in all the other cases. Further work by Lee et al. [84] built on this using an elasto-viscoplastic self-consistent (EVPSC) approach enabling interpretation of neutron scattering measurements of texture during deformation of Mg-9 wt%Al. This EVPSC model was found to best agree during elastic unload, rather than through the loading history, which implies that texture is well represented but the mechanisms leading to significant crystal reorientation during twinning are not.

Experimental studies on the morphology of deformed polycrystals which exhibit significant twinning have been undertaken largely with EBSD, which enables twinning populations to be studied relatively quickly and the twin types identified readily using misorientation axis/angle relationships. Capolugo et al [85] demonstrate effective use of EBSD in performing a statistical study of nucleation and growth of twins in Zr and in particular correlated $\{10\bar{1}2\}$ twins formed at 77K with crystal

orientation. This experimental study highlights problems with deterministic approaches that drive twinning to be modelled using a predominant twin system (PTS), as this limits twinning to only one twin variant per grain and that instead the local stress state within each grain will drive twin *nucleation*, whereas twin *growth* broadly can be modelled using an average (i.e. macroscopic) stress state per grain.

Ghaderi and Barnett studied the effect of grain size on twinning in Mg and Ti. In Mg, for constant strain, the twin volume fraction is almost insensitive to grain size while in Ti twins are more likely with larger grain size [79]. Furthermore, they show that increasing grain size in Mg increases the number of number of twins per grain and in Ti this effect is far stronger. This highlights that *nucleation* is a significant limiting factor in the micromechanisms of twinning, as in larger grains the slip length is larger and therefore the total stress heterogeneities associated with grain boundaries are presumably larger. Furthermore, in small grain titanium alloys a twin can completely consume and reorientate a parent grain [86]. Ghaderi and Barnett [79] noted that in large grain material the twins do not necessarily extend the full length of the grain. It is therefore important to understand what can terminate a twin and accommodate the significant strain heterogeneity associated with the head of a twin.

Ghaderi and Barnett's study [79] complements work of Beyerlein et al [87] who applied statistical approaches using EBSD to study twinning in Mg. Beyerlein et al [87] highlight the importance of local stress states and that the orientation of the twinned grain with respect to the applied load has significant statistical variability and that pair statistics, i.e. including the grain neighbourhood, must be included. Beyerlein et al [87] discuss differences between Mg and Zr and comment that if Zr requires higher stress concentrations for nucleation then prior slip activity near the grain boundary (the twin nucleation region) is of utmost importance in predicting local stress intensity. The discrepancy between the deterministic CRSS for twin nucleation and an effort to capture probabilistic effects included in the precise dislocation and twinning dislocation reactions at the grain boundary led Beyerlein and Tome to develop a probabilistic modelling approach [88]. This approach is more suited when considering the competition between, for instance, <a> prism slip and $\{10\bar{1}2\}$ twinning in Zr at low strains, and more reasonably captures the onset of twinning, rather than prior studies which broadly only capture the effect of twinning on the hardening response (caused by grain reorientation and mean free path reduction due to grain segmentation).

Methods to properly capture the local stress state with crystal plasticity simulation have been performed, typically including twinning as a pseudo-slip mode, but in contrast to self-consistent approaches the local stress state from grain-to-grain compatibility and equilibrium is more properly captured. Abdolvand and Daymond [89, 90] present a multi-scale study simulation route that has roots in the self-consistent schemes, enabling twins to form once the twinning strain (accumulated on all variants) exceeds a critical inception value (akin to twin *growth*) and the properties of the integration point are updated to reflect the new orientation of the twinned material. This necessarily causes significant numerical instability in the solver (the twin can reorient the crystal by 85°, and therefore significantly change the crystal stiffness). Once the integration point is reoriented alternative twinning mechanisms are deactivated and the twin deforms as if it were a newly created grain (i.e. accumulated slip and hardening is forgotten and it has reoriented elastic properties). This model has many different free parameters (eg CRSS for each slip mode, hardening parameters from the Voce scheme, CRSS and hardening for each twinning mode and the critical value for inception).

Therefore calibration was performed using deformation of 3D voronoi tessellations of grain structures and compared with experimental EBSD maps (where available) and surface strains measured with DIC. This simulation strategy performed well in broadly capturing consistent trends between experiment and simulation, highlighting that local stress states are important rather than the globally imposed loading scheme (although clearly this has an impact with respect to the texture of the sample). One particular highlight of this work is to reasonably predict the location of grains with active twinning modes.

Twinning is a complex process and the geometry of microstructures extends beyond two dimensions. There are exciting developments using high energy X-ray facilities, including HR-XRD and 3D micro-Laue diffraction to draw out these effects.

Wang et al [91] combined EBSD with Laue microdiffraction to study deformation around T2 $\{11\bar{2}1\}$ twins in Ti and investigated sub-surface dislocation structures associated with twin thickening and suggested that <c+a> dislocations transmute from a pyramidal plane to a prismatic plane within the twin. Bieler et al [92] used 3D XRD to study $\{10\bar{1}2\}$ twinning in Ti and extracted average (grain centroid) strain from far-field measurements. One grain, surrounded by hard grains, activated twinning on the expected (from macro-loading) plane; however in two other grains, surrounded by softer neighbours, the activated twinning was not on the plane with the highest resolved shear stress and the authors attributed this to slip-stimulated twinning from the grain neighbourhood. Here *in-situ* methods enabled direct measurement of the local stress state and provides some of the first evidence on load partitioning between twin and parent which indicated that the twin had ~30% less stress within it.

Aydiner et al. [93] used 3D high energy X-ray diffraction to study the stress states within the twin and parent grains of a large grain Mg alloy in compression, where the $\{10\bar{1}2\}$ tensile twin was activated. Resolution of the stress state of twin and parent revealed significantly different shear stresses, attributed to the constraint of the twin domain inhibiting deformation and leading to an increased back stress in the parent grain.

Lynch et al. [94] used a sophisticated 'single shot' 3D Laue diffraction method to capture the spatial and temporal dynamics of twinning in a Mg alloy (AZ21). Twinning followed the activation of basal slip. After the twin nucleates, twin growth continues to increase the diffraction intensity from the twin orientation, representing a change in twin volume and twin shape. Further analysis indicates that there is accommodation of strain by additional dislocation slip. Analysis of the stress states before and after twinning indicates that in AZ21 the basal CRSS is 18 ± 3 MPa and the twinning CRSS is 23.5 ± 5MPa and twin growth occurred with resolved stresses of between 5 and 7MPa.

These studies indicate increased complexity when addressing critical resolved shear stresses for twinning operations (deformation prior to twin nucleation, twin nucleation and twin growth) and motivates models to consider twin initiation and growth differently.

6. Polycrystals and Boundaries

In this section, we progress from our focus on single crystal behaviour towards addressing understanding of polycrystalline HCP alloys and their behaviour under conditions relevant to their in-service loading. We restrict the focus to the titanium alloys which find widespread usage in

engineering applications. The section begins with an assessment of micro-deformation and the rôle of grain boundaries, $\alpha-\beta$ phase distributions and interfaces and tension – compression asymmetry. An important aspect of the titanium alloys is that they show rather remarkable creep, relaxation and strain-rate sensitivity behaviour even at relatively low (eg 20°C) temperatures which, it is argued, is important in understanding their response to in-service loading and this is addressed subsequently. The important phenomenon of cold dwell facet fatigue is then addressed, and finally, the more general aspects of fatigue and crack growth are considered.

6.1 Polycrystal Ti behaviour and the rôle of α-β interfaces and grain boundaries

Much highly insightful work has been carried out in elucidating the behaviour of titanium alloys by Mills' group [69, 70, 95-99] and a particular highlight was the conclusion that much of the observed behaviour resulted from the establishment of a Burgers Orientation Relationship (BOR) between the α phase HCP orientation and the adjacent transformed β phase (BCC) orientation, shown schematically in

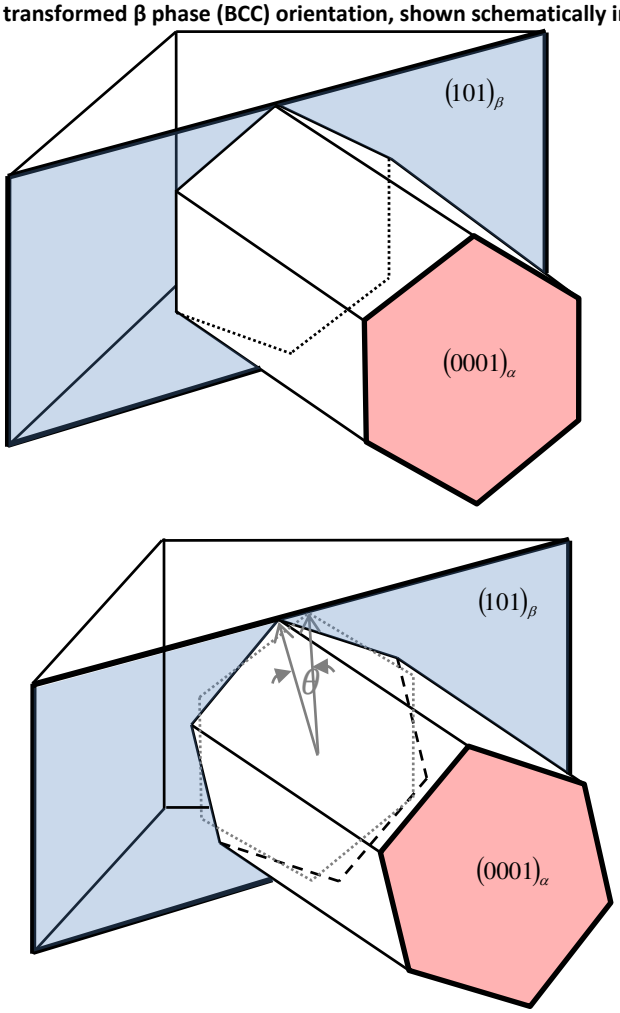

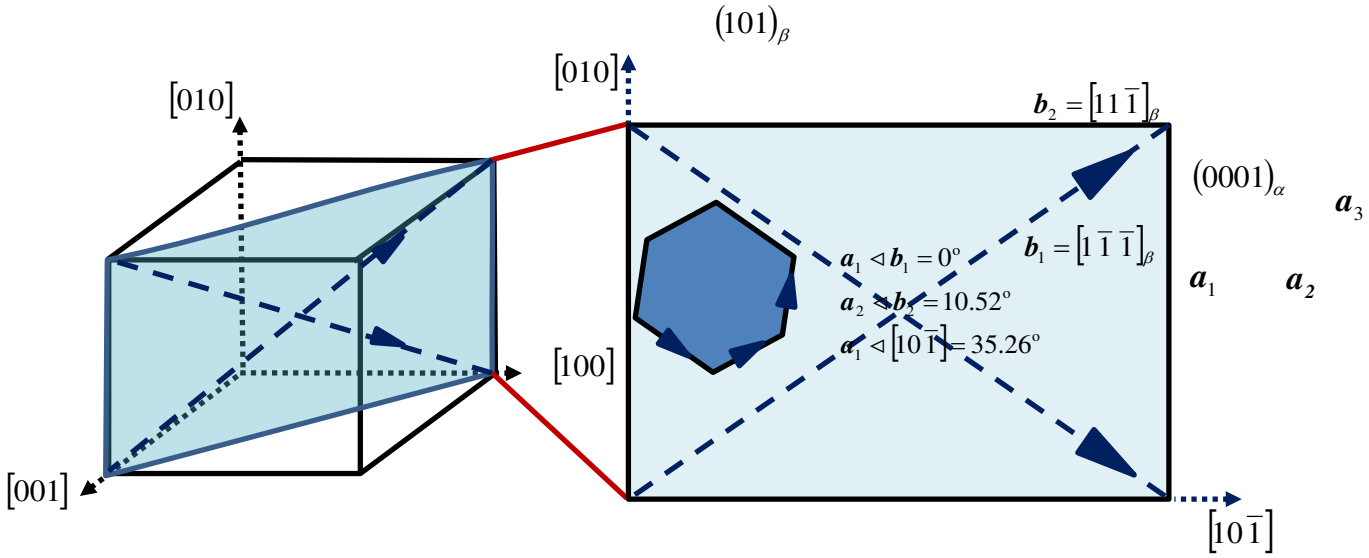

Figure 8(a), and with quantitative detail for a coherent interface in

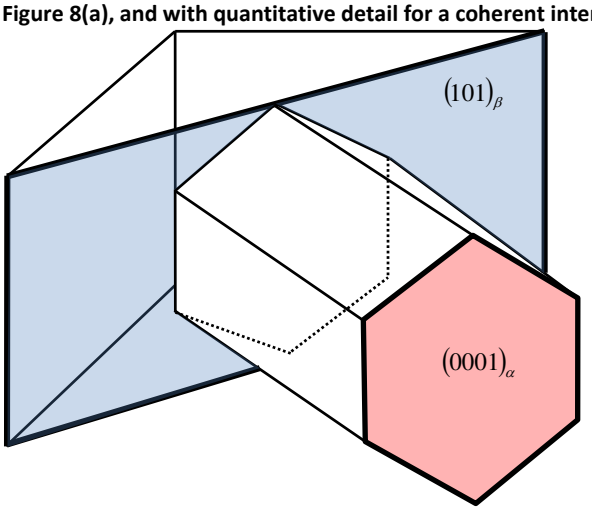

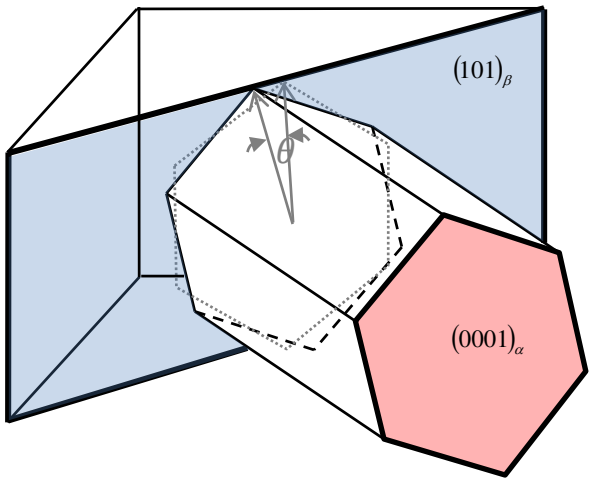

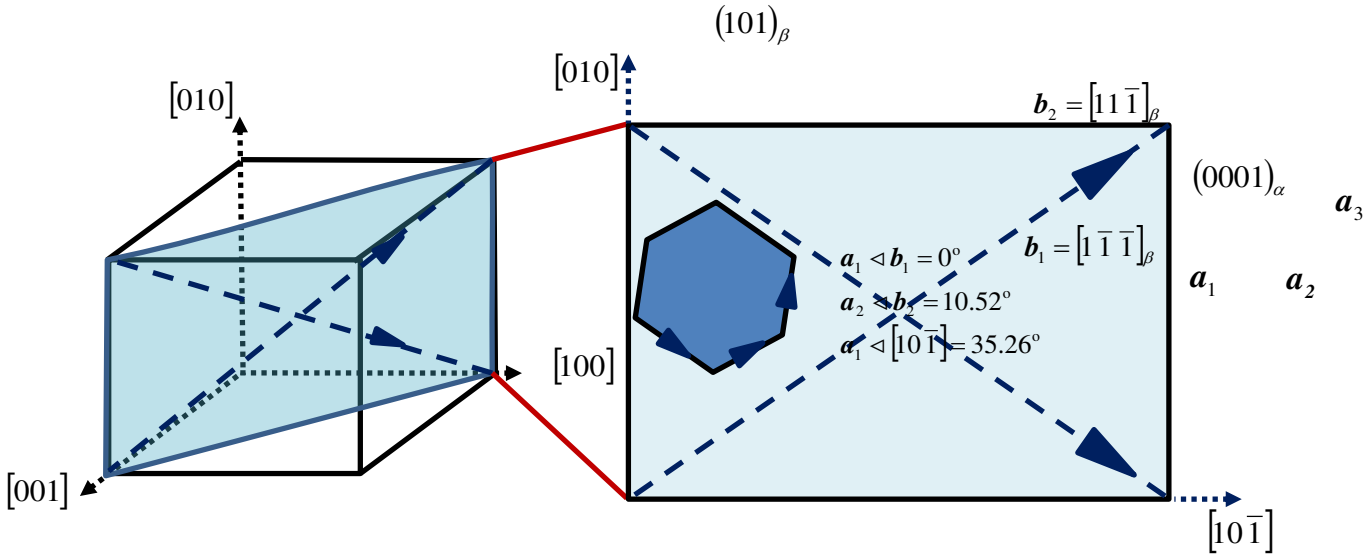

Figure 8(b). This can be described through the common closest packed planes shared between the two phases $(101)_\beta \| (0001)_\alpha$ **as well as the sharing of close packed directions** $[1\bar{1}\bar{1}]_\beta \| [2\bar{1}\bar{1}0]_\alpha$ **shown in**

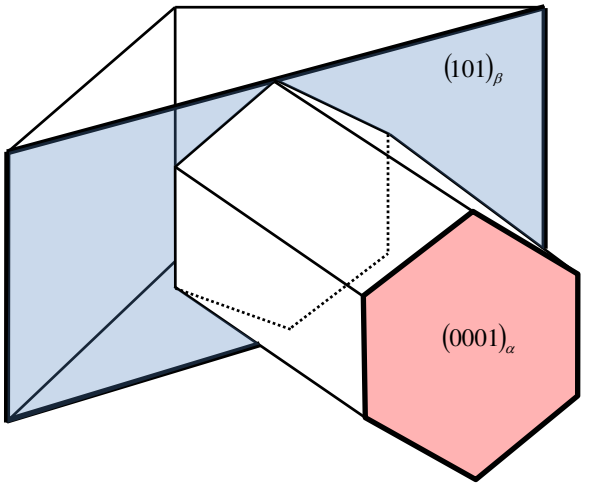

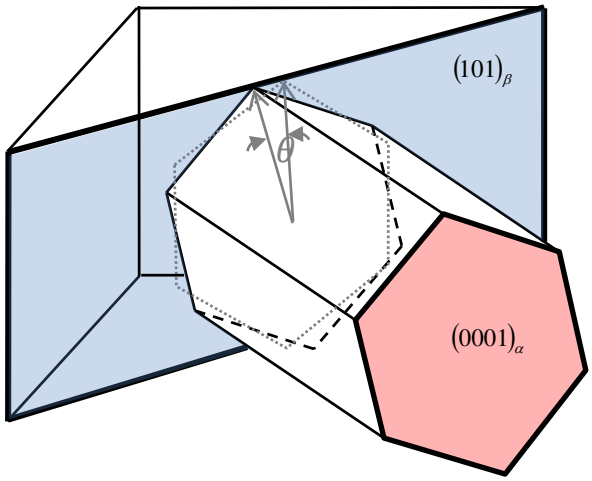

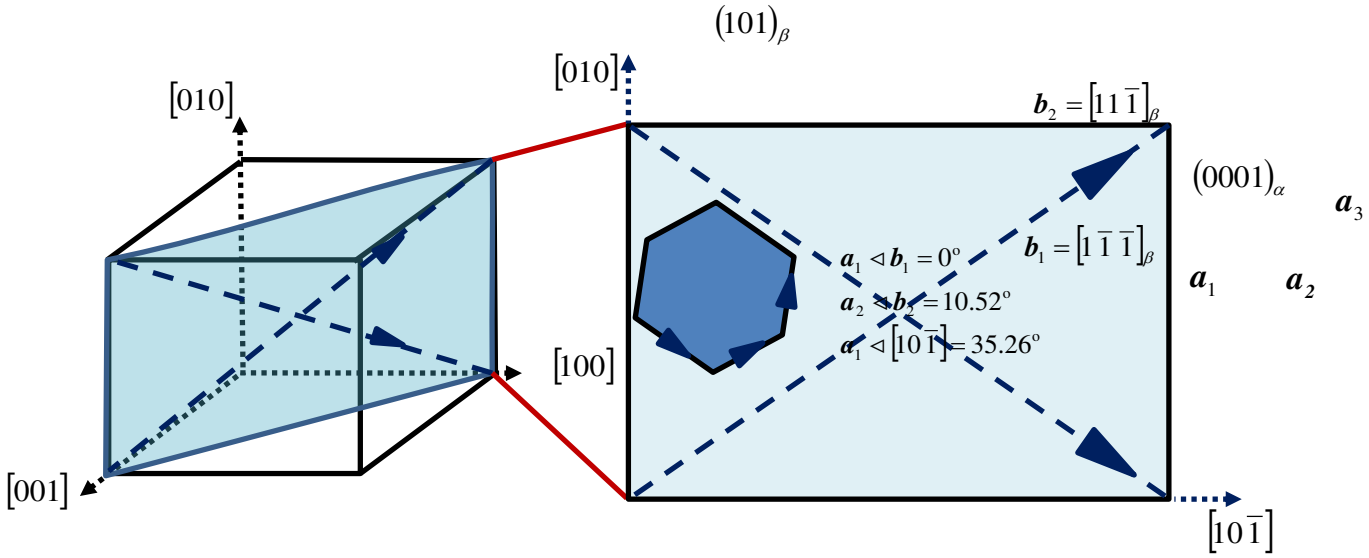

Figure 8(b). The β phase has six $\{101\}$ planes on which up to 12 daughter α variants may form. Furthermore, the BOR only has one direct overlap of close packed directions between the two phases, indicated with an <a_1> Burgers vector

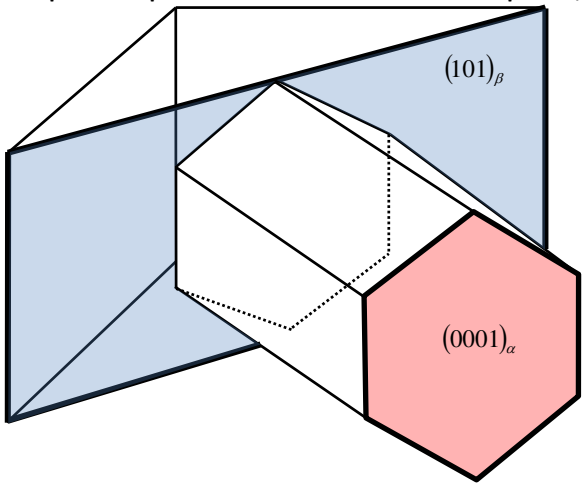

(aligned with <b_1> in

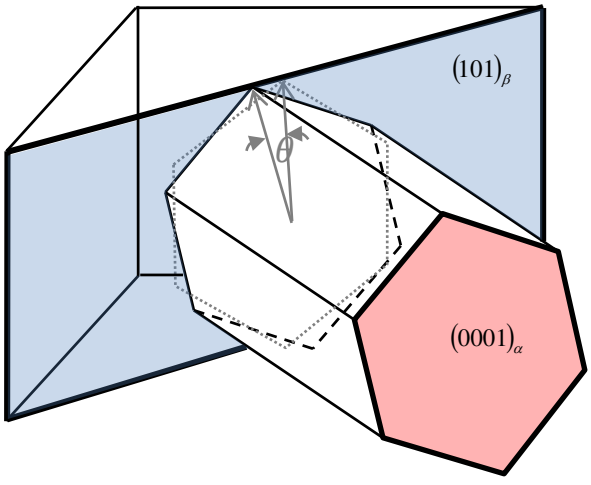

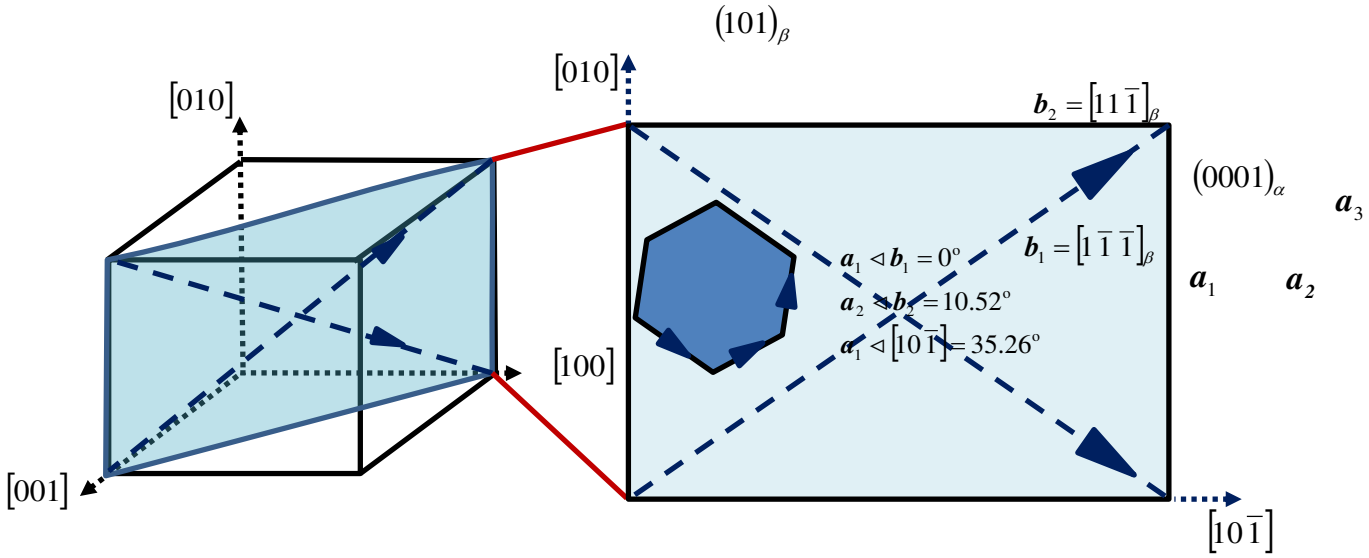

Figure 8(b)). The <a_2> direction is closely aligned with the <b_2> direction in the parent (111) plane, with typical misalignments of ~10° or more. The <a_3> direction does not map onto a Burgers vector in the β phase, and the closest vector is a <b_3> direction pointing along one [100] direction. In practice, some misalignment from the ideal BOR is found to exist in many alloys, leading to an incoherent interface, which is shown schematically in

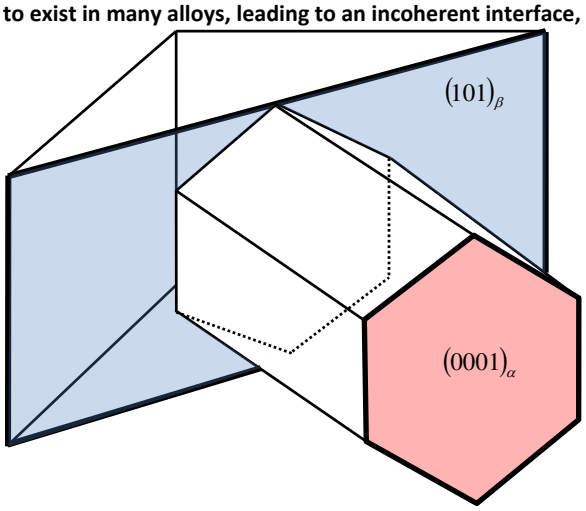

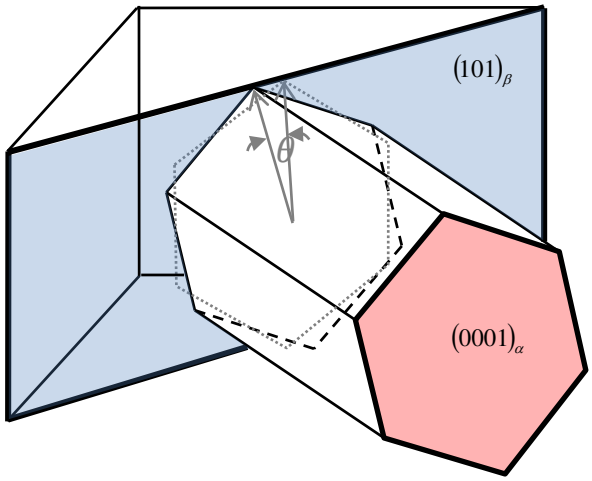

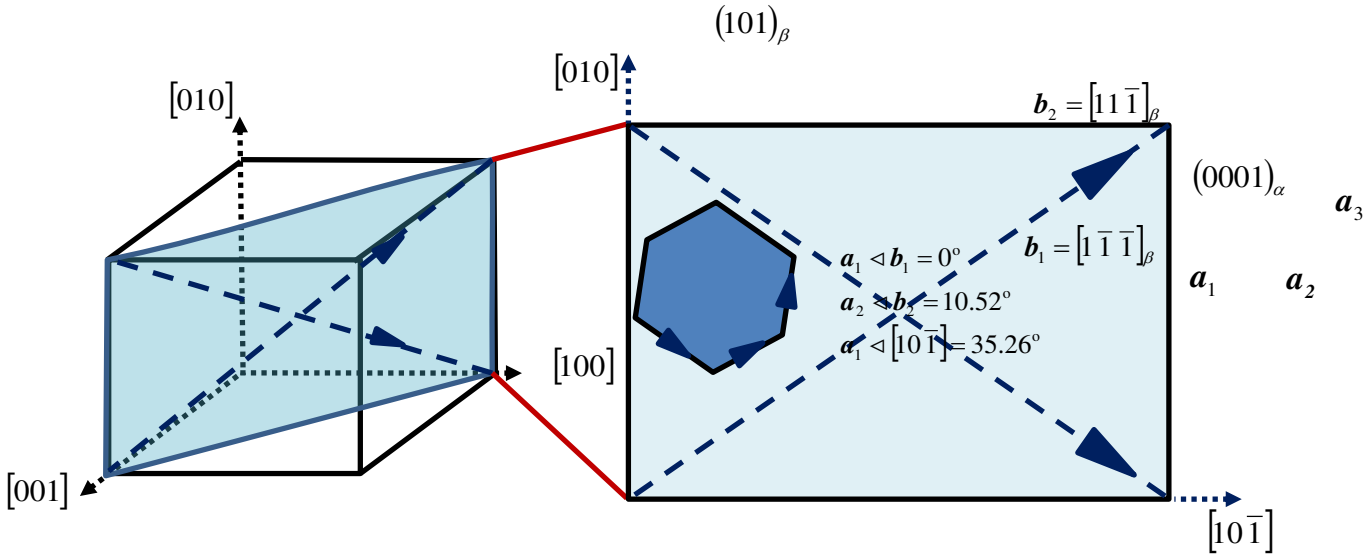

Figure 8(c), in which a rotation of angle θ about the alpha HCP c-axis is shown, resulting in the loss of colinearity between the alpha <a_1> $[2\bar{1}\bar{1}0]_\alpha$ direction and the adjacent beta <b_1> $[1\bar{1}\bar{1}]_\beta$ direction. Coherent interfaces only are considered further in what follows, but alpha-beta variant selection has been addressed recently in detail by Shi et al [100].

Suri et al [95] addressed in particular the creep response of two phase α–β alloys and carried out creep tests on single colony near-α alloy comprising a majority of α phase with β laths observable within the sample faces. With reference to

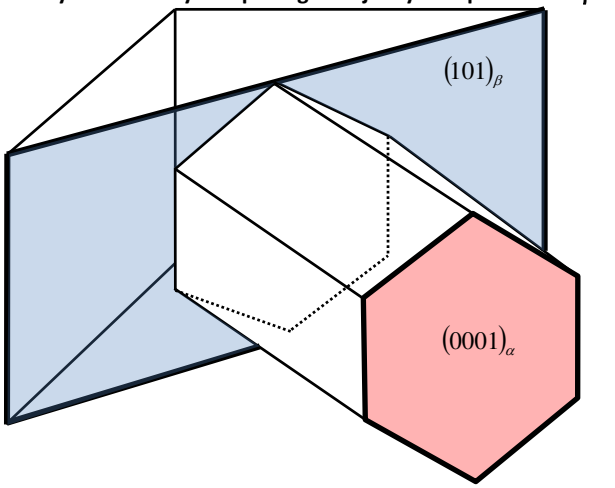

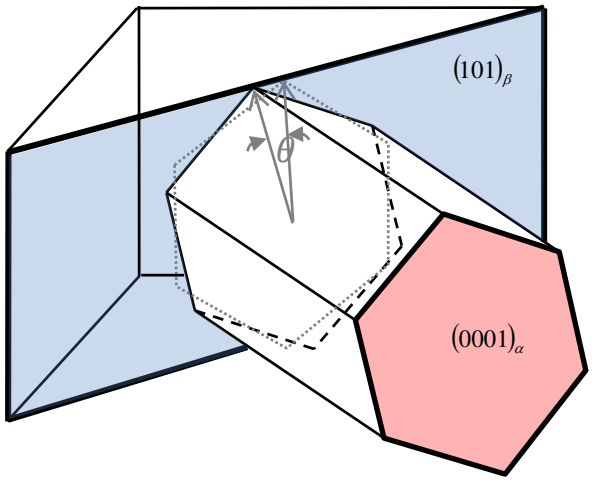

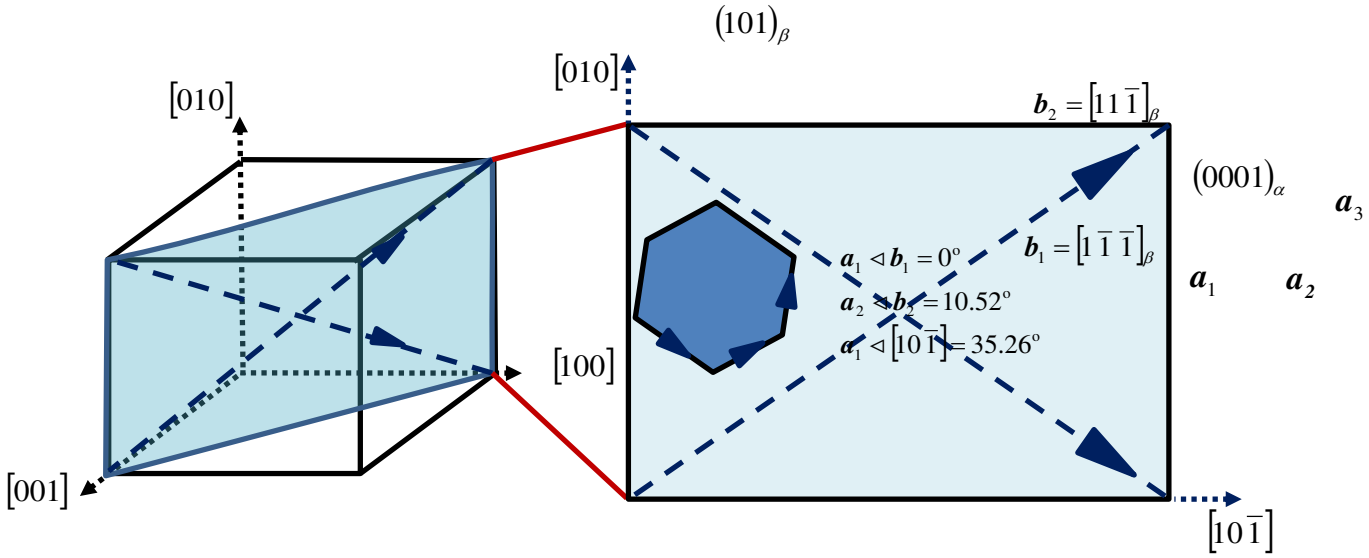

Figure 8(b), two loading configurations were examined by Suri et al in which the highest resolved shear stress was arranged to be acting on the <a_1> and <a_2> prismatic systems respectively. The latter gave rise to <a> slip near-normal to the α–β interface resulting in higher macroscopically observed yielding and hardening, in agreement with Chan et al [101]. In addition, a colony configured for <a_1> prismatic slip gave creep rates three orders of magnitude higher than that configured for <a_2> slip, and intense planar shear bands were observed running through the β laths; sheared regions were also observed in the α phase at the entry and exit locations adjacent to the β lath, showing planar slip attributed to short range order (SRO). Short range order here refers to local structure that affects dislocation planarity, but it is not clear over what range this order persists.

Ordering of Al atoms was assessed in alloy Ti-6Al [70] and found to lead to the preferential development of planar slip, together with significant strengthening in creep. It is believed to result from the presence of a fine Ti_3Al precipitate in the primary α phase, resulting in uniformly spaced slip traces across the entire α grain. The absence of SRO in material, ice water quenched from the 900° homogenisation temperature, led to homogeneous slip and the inhibition of planar slip. Suri et al [95] argued that slip transmission across the α–β interfaces in near α Ti-5Al-2.5Sn-0.5Fe is strongly dependent on the <a> system orientation with respect to the interface, in the context of the BOR. Furthermore, they did not observe interface sliding. Ankem and Margolin had earlier argued that α–β interface sliding had been observed at room temperature under constant strain rate loading [102]. Colonies oriented for <a_1> slip showed no edge dislocation pile-up and the α–β interface showed little resistance to slip transfer. However, colonies oriented for <a_2> showed much edge dislocation pile-up at the α–β interfaces and a correspondingly much higher resistance to slip transfer. Ambard et al [103] subsequently examined interphase α–β deformation in Ti-6Al-4V at 20K and at this cryogenic temperature observed that basal slip dominated in the colony α laths, but that prism slip dominated in the equiaxed α phase regions. This implies that difficulty in slip transfer across beta laths reduced long range prism slip (i.e. between α phase packets), at least for the cryogenic temperatures considered. In passing, while, Feaugas and Clavel [104] had earlier shown in Ti-6Al-2Sn-4Zr-6Mo under cyclic loading that slip was predominantly accommodated by <a> prism activity and they also observed some <c+a> slip early in the cyclic history.

Further work by Savage et al [98] established that the $\alpha-\beta$ laths in Ti-6Al-2Sn-4Zr-2Mo maintain approximately the BOR and single-colony tests indicated the inhibition of slip transmission for systems in which the α HCP phase was well-orientated for basal slip. β lath shearing was inhibited in these circumstances, but not so for orientations favouring prism slip. Savage et al [105] subsequently addressed creep recovery in $\alpha-\beta$ colony structures and again observed planar slip attributed to SRO, with little dislocation interaction between the slip bands (Figure 9). The slip bands impinging on grain boundaries (GBs), and an example is shown in Figure 9, were argued to cause very significant stress concentrations and the dislocation orientation was found predominantly to be mixed near to the GB and largely screw away from the boundary.

More recent work by Britton and Wilkinson [106] in single phase commercially pure titanium has quantified the stress concentration generated by a slip band impinging on a grain boundary using high-resolution EBSD. This approach was exploited further by Guo et al [107] who examined multiple examples of slip bands impinging on grain boundaries. They found three broad categories of behaviour: (i) blocked slip bands leading to intense stress concentration where slip system alignment across the boundary was poor, (ii) slip transfer with negligible stress concentration when slip system alignment was good, and (iii) blocked slip band with negligible stress concentrations when slip system alignment was intermediate.

The planar slip observed by Savage et al [98] also occurs near $\alpha-\beta$ interfaces in single-colonies and the stress concentrations which develop at the interfaces were relieved by room-temperature creep processes. They argue also that room temperature creep has not been demonstrated in β Ti, so that the dislocation pile-ups in β laths do not lead to relaxation and hence the absence of observed creep recovery in colony samples orientated for $<a_2>$ basal slip. They conclude that large pile-ups of $<a_2>$ dislocations must exist in the α phase in order for significant recovery to occur.

Tests were subsequently carried out on Ti-6Al-2Sn-4Zr-2Mo by Savage et al [97] orientated in such a way to generate $<a_1>$, $<a_2>$, or $<a_3>$ slip within different single colonies with the α region adjacent to β laths in which a near-BOR between the $\alpha-\beta$ phases exists. In the sample orientated for $<a_1>$ basal slip, relatively easy slip transmission occurs across β laths. No pile-ups are observed at interfaces, suggesting stress concentrations are not required to generate slip transmission. However, for basal $<a_2>$ and $<a_3>$ slip systems adjacent to β laths, higher resistance to slip and stronger strain hardening are observed to occur in single colonies. For $<a_2>$ basal slip, no dislocation pile-ups are observed at $\alpha-\beta$ interfaces, but for thicker β laths, dense pile-ups of dislocations are observed at the exit $\alpha-\beta$ interface, suggesting relatively easy $<a_2>$ transmission within the β phase, but difficulty in exiting of $<b_2>$ dislocations from the β phase at the $\alpha-\beta$ interface. For $<a_3>$ basal slip, large pile-ups of near-edge $<a_3>$ dislocations are observed in the α phase at the $\alpha-\beta$ interfaces, showing the large resistance to slip developed at the β laths for $<a_3>$ basal slip.

Tension-compression asymmetry in creep was examined by Neeraj et al [96] in Ti-6Al and Ti-6Al-2Sn-4Zr-2Mo alloys; and they found that in Ti-6Al under compression, <a> type slip was observed to be widespread together with some <c+a> activity near grain boundaries, but under tensile load, no <c+a> activity could be observed. Observations of <c+a> slip activity were also made by Medina Perilla and Gil Sevillas [108] near grain boundaries in Ti-6Al-4V, supported by TEM observations. Earlier work by Jones and Hutchinson [109] in highly textured Ti-6Al-4V deformed along $[0001]$ to generate mostly <c+a> slip showed a ~40% higher CRSS value in compression than in tension, with

clear evidence of cross-slip away from the $\{10\bar{1}1\}$ pyramidal plane for the compression case. Similar observations were made on micro-cantilever samples recently by Ding et al [110]. In Ti-6Al-2Sn-4Zr-2Mo single colony tests orientated for <a> basal slip in compression [96], planar (SRO) slip occurred which was highly heterogeneous, but tensile loading generated very homogeneous slip in the same $<a_1>$ basal systems as activated in compression, with the same occurring for $<a_2>$ and $<a_3>$ basal slip, indicating that cross-slip was much more active in tension than compression for all three basal systems. The authors argued that the <c+a> slip could not explain the tension-compression asymmetry, but rather, hypothesize that it results from non-planar <a> type screw dislocations on first order pyramidal planes, making the screw dislocation sensitive to applied stress direction, and explaining the higher propensity for cross-slip on pyramidal planes in tension, similar to non-Schmid behaviour in BCC metals.

Some work has been carried out in order to develop modelling capability at the grain-scale in the alloys discussed above. Zhang et al [111] as well as Mayeur and McDowell [112] employed crystal plasticity for alloy Ti-6Al-4V to represent explicitly the duplex primary α phase together with lamellar $\alpha+\beta$ colony regions in which the BOR is recognised and included. The models provided the ability to examine the sensitivity of the resulting macro-scale material response to the details of the microstructure (eg slip system strengths) to be assessed. A systematic study of combinations of crystal orientation embedded within a model Ti-6Al alloy by Dunne et al [113, 114] utilized a crystal plasticity model which incorporated creep and stress relaxation. They showed that grain boundary stress states depend strongly on misorientation such that local slip accumulation is hugely inhomogeneous and that a 'worst case' combination of orientations exists leading to the highest grain boundary stresses. Subsequently Dunne et al. demonstrated techniques for extraction of geometrically necessary dislocation (GND) density from crystal modelling of HCP polycrystals [115] and showed representative GND activity for <c+a> slip to be an order of magnitude smaller than that for <a> type slip, in agreement with the experimental observations of Britton et al [116] and Littlewood et al [117, 118]. Self-consistent polycrystal modelling was employed by Warwick et al [119, 120] in order to interpret neutron diffraction measurements of elastic strain partitioning in Ti-6Al-4V and to attempt to extract slip strengths for the differing slip systems. However, self-consistent approaches ignore crystal morphologies and interactions, and abandon the requirement either for strain compatibility or for equilibrium. These are severe limitations, and are likely to be important when attempting to calculate local properties and behaviour such as slip strengths and load sharing between grains and neighbouring phases.

The room temperature creep response of many Ti alloys has already been referred to above, and because of its importance in determining in-service behaviour and performance of engineering components, this together with the related phenomena of stress relaxation and strain rate sensitivity, are addressed explicitly in the next section.

6.2 Creep, relaxation and strain-rate sensitivity in Ti polycrystals

It is now well established that a range of titanium alloys show strong strain-rate dependence, creep and stress relaxation behaviour even at low homologous (T/T_m) temperatures of 0.15, corresponding to room temperature, and that their overall properties and performance are influenced, potentially very strongly, by this behaviour [69, 95, 105]. For example, the room-temperature creep response of Ti-6Al-4V alloy has recently been described phenomenologically by Harrison et al [121]. Some work has been carried out to examine the mechanistic basis of the time-dependent response in colony

structures, and several authors have argued its significance in the phenomenon of cold dwell fatigue. Therefore creep relaxation is fundamentally important to the behaviour of alloys in service, though the origins of the creep-like behaviour at temperatures of 20°C and lower remain elusive.

The $\alpha-\beta$ colony studies of Suri et al [95] addressed creep in a near-α alloy and showed that the creep rates in the α laths depended strongly on the BOR <a> type slip orientation with respect to the adjacent β laths. Neeraj et al [69] demonstrated the rate sensitivity of alloys Ti-6Al and Ti-6Al-2Sn-4Zr-2Mo, and Savage et al [105] demonstrated creep relaxation in the α phase. Cold dwell fatigue is here considered to be the development of material separation over a grain or region of uniform crystallographic orientation of whatever size and is addressed later, but it is relevant in passing to note that the room-temperature creep and relaxation behaviour is hypothesised by several authors to be an important mechanism for the facet nucleation process in cold dwell fatigue. The first study to demonstrate the phenomenon of load shedding was presented by Hasija et al [122] in which it was shown, using crystal plasticity modelling, that the creep response at the single-crystal level, under conditions of load hold, led to the redistribution of stress from a grain well-orientated for slip on to an adjacent grain which was badly orientated for slip. Typically, the badly orientated grain was such that its basal plane was approximately normal to the applied (macroscopic) loading (Venkatramani et al [99]). Crystal plasticity models for near-α Ti alloys which incorporate strain-rate dependence, creep and stress relaxation were also developed by Dunne et al [113, 114] and Rugg et al [123] explained why load holds in the cold dwell regime are more damaging then strain holds, because of the differing modes of stress relaxation occurring, and as observed in experiments.

6.3 Cold dwell facet nucleation, fatigue and crack growth in Ti polycrystals

Dwell fatigue is where a hold under load during cyclic loading results in a significant reduction in the number of cycles to failure compared to cycling without the hold. The term cold dwell fatigue in titanium alloys is thought to have arisen firstly, by virtue of the debit to fatigue life observed by incorporation of the *load-hold* within the fatigue cycle, and secondly because the formation of micro-cracking occurred in aero-engine components operating typically between -40 to 200°C (233 K to 473 K); a temperature range which is lower normally than has been associated with dwell, or creep effects in high-performance alloys. The early occurrences and investigations were in engine discs (i.e. large size and material volumes, quite different from those associated with laboratory-based tests), and it is useful to note that the phenomenon of cold dwell was, and remains in the aero-engine industry, associated with the formation of facets, sometimes described as quasi-cleavage because of the absence of any evidence of substantial plasticity on the facet surface. The facets in discs were typically found on basal planes in regions of uniform crystallographic orientation (sometimes referred to as structural units, or macrozones), and the basal planes were typically orientated within +/-10° of the macroscale maximum principal stress direction. A further important feature of cold dwell in Ti disc components is that the resulting stress – cycles to failure (S-N) curve is very flat (and extraordinarily expensive to establish, with each point requiring a full scale over-speed disc test to failure). An important consequence is that the component design criteria are therefore such that permitted stress levels have to fall below that for facet *nucleation*. As a consequence, facet nucleation is deemed to be the life-limiting process, and not subsequent facet growth [124].

Reproducing the service-like phenomena of large scale engine discs at the laboratory scale has remained difficult. This could be due to of the limited volume of material within moderately sized specimens, and therefore the range of crystal orientations and local misorientations is not sufficient.

It is observed that increased applied stresses are required in order to generate facets in the laboratory, possibly because weakest link combinations of grain misorientations are less likely to occur in limited volumes. Furthermore, in laboratory tests a much wider range of faceted basal orientations with respect to the macro-loading direction has been observed. It therefore remains an open question whether the mechanistic basis of the facet generation in laboratory tests is the same as that which occurs in larger volumes associated with discs. Further complications arise from many important variations in titanium materials, such as the rôle of the α-β colonies and morphologies, chemistry, and several others (eg SRO). Indeed, recent attempts at larger-scale laboratory-based tests with representative sample diameters of 50mm have still not provided a persuasive link to disc-scale facet behaviour [124].

Much research in cold dwell was carried out by the Evans and Bache group [125] and one of several legacies from that work was the proposition that the Stroh model [126] for a line of dislocations within an infinite isotropic, elastic medium orientated to remote uniform, uniaxial stress, could explain the development of high stress at the termination of a slip band impinging on a boundary between two HCP α units, one well-orientated for slip and containing the slip band, and the other orientated to inhibit slip. This idea supports a local combination of crystallographic orientations as a stress raiser required for basal facet formation [125]; however it does not address nor explain the time sensitive, i.e. dwell, dependence.

Lefranc et al [127] investigated dwell fatigue in Ti-6Al-2Sn-4Zr-2Mo with an $\alpha-\beta$ colony structure and observed crack nucleation by coalescence of shear-induced cavities which nucleated at the $\alpha-\beta$ interfaces in the large colonies of α laths which were near-parallel to the (macroscale) loading axis. The density and size of cavities were larger under dwell fatigue conditions, but it is important to note the relatively high applied stress in this study, close to or exceeding macro-level yield. Shear-induced microcracks from cavities at $\alpha-\beta$ interfaces were also observed by Gerland et al [128], but again for applied stresses in excess of yield. It was argued that creep could be inhibited by the presence of hydrogen (at a concentration of about 300ppm) which resulted in a beneficial influence on dwell fatigue life, and so far as the authors are aware, this is the only experimental study which explicitly demonstrates a link between inhibition of grain-level creep and extension of dwell fatigue life, reinforcing the Hasija et al [122] load shedding hypothesis in cold dwell. In passing, Gerland et al [128] note that most of the hydrogen resides in the β phase, but that it could be transported to the heavily deformed α laths.

EBSD studies in colony $\alpha-\beta$ Ti-6Al-4V were utilized by Bridier et al [129] to examine the crystallography associated with critical damage and failure. Basal plane cracking was found to occur earlier and to be more rapid than for prismatic planes, and crack formation was found to be promoted in macrozones (Germain et al [130, 131]) with (0001) basal plane texture normal to the tensile axis. EBSD studies in IMI834 were carried out by Uta et al [132] which identified crystallographic domains, or macrozones, with near-uniform orientation, which had a band-like structure. Crack nucleation sites under cold dwell conditions were found to contain numerous 'quasi-cleavage' facets, and the nucleation zones were found to have α <c> axes within 30^o of the (macro-level) loading direction. The samples tested were representative of disc material but of small size (6mm diameter) and at 85% of the macroscopic yield stress. However, primary facets were found to be close to basal planes. Bridier et al [129] investigated crack nucleation in Ti-6Al-4V under standard (i.e. non-dwell) fatigue under strain control (ε_{max}=0.8%, R=0). The alloy considered

comprised about 40% globular primary α and 60% lamellar α-β structures, but crack nucleation occurred in the primary α globules, originating from both prismatic and basal systems, though the propagating, most damaging, cracks all originated from basals. While basal crack nucleation was associated with moderate Schmid factors, no evidence was seen of cleavage-controlled basal cracking; that is, plasticity was found to be important for both basal and prismatic crack nucleation in these (non-dwell) fatigue studies.

Failure in materials at microstructural length scales must include resolution of stress and strain states onto individual crystals, and the effects of grain neighbourhoods which may change the principal stress and strain directions in anisotropic materials. These length scales can extend to many millimetres in titanium alloys, due to the presence of macrozones or effective structural units with common crystallographic orientations that extend through the alpha phase in thermo-mechanical processed materials. Resolution at the microstructural length scale results in changes between global and local calculation of factors used to correlate with damage and failure, due to inherently anisotropic mechanical responses. This relates to dwell fatigue also, where knowledge of local, grain-level stress and strain components are the relevant quantities, which may be quite different to the macroscale applied stress state,. In practice these local effects can lead to deviations of the principal axes from the macro-level loading direction by as much as 30^{o}. This is especially true when considering titanium alloys, where microstructural units may extend over a very large fraction of a laboratory scale sample and limit statistical representation, in microstructure as well as applied stress and strain states, of full component samples. These effects can and are routinely captured in crystal plasticity modelling efforts, where elastic and plastic anisotropy as well as grain structure is included as a matter of course.

Crystal plasticity modelling work to address the rôle of grain-pair combinations of crystallographic orientation and basal plane orientation was carried out by Dunne et al [113, 114] in which near-α alloy Ti-6Al was considered. Unlike the Stroh analysis [126], the full incorporation of elastic and slip anisotropies along with time dependent plasticity within a model oligocrystal allowed systematic studies of crystal orientation and grain-pair orientations and showed that a worst case in this system does exist in which a grain well-orientated for slip has an active slip system orientated at about 30^{o} to the direction of the adjacent hard grain <c> axis; this combination leads to stress concentrations near the grain boundary which are the highest, and in particular, the highest stresses normal to the hard grain basal plane occur when this basal plane is orientated normal to the maximum principal stress.

The first rigorous analysis and explanation of the effect of dwell was presented by Hasija et al [122] who explained the phenomenon of load shedding (see section 6.2 above), resulting from the room-temperature creep response of some Ti alloys, and linked it to the experimentally observed dwell dependence of the fatigue lives. The experimental observations of Gerland et al [128] at the grain level support this hypothesis. The crystal plasticity models of Dunne et al [113, 114] and Rugg et al [123] also incorporated creep and stress relaxation effects and demonstrated the differences in local, grain-level stress relaxation resulting from macro-level stress-hold loading as opposed to strain-hold loading, with the former leading to considerably higher load shedding on to the hard grain. Subsequent analyses [133, 134] included a cleavage criterion based on single crystal <c> direction tensile strength in which a range of differing microstructural representations (including worst case orientation combination and others) and loading states were assessed for propensity to

generate facets. The experimental observations of Sinha et al [135] and Bache et al [134] were successfully reproduced. Kirane and Ghosh [136] proposed a nucleation model recognising the development of localised slip resulting in stress concentration at the hard – soft grain boundary but based on a local critical stress intensity. Subsequent work by Anahid et al [137] allowed for the development of local dislocation density arising from multi-slip. Other work in crack nucleation (but in bcc polycrystals) addresses local, microstructure-level quantities including accumulated slip, dislocation density, stress and a local (Griffith-like) stored energy in order to reconcile experimentally-observed crack nucleation sites [138], and such approaches may have potential for cold dwell facet nucleation.

Relatively recent work by Pilchak and Williams hypothesised that hydrogen played a rôle in facet formation [138], reflecting the earlier work of Gerland et al [128]. An alloy comprising globular α and 35% $\alpha+\beta$ colonies was examined. Dwell fatigue samples tested at 95% of the macroscopic yield stress exhibited sub-surface nucleation, and facet initiation in this work was considered to be the formation and progressive linkage of facets across uniform regions of α phase, and not an instantaneous formation in a nucleation sense. The initiating facet was less that 1° away from the basal plane but the crystal <c> axis was determined to be 43° to the macro-level loading direction. In the absence of worst case combination of crystallographic orientation and $\alpha-\beta$ lath morphology, arising in small volume laboratory-based tests, crack nucleation may well be forced to occur in less badly arranged grain configurations, often at higher loading regimes, and an example is given by Bache et al (2010). In later work, Pilchak [139] adopted a macro-level stress intensity range approach for facet growth, but does not address explicitly first facet nucleation, which in many ways is the key life-determining process for engineering components undergoing cold dwell.

McBagonluri et al [140] examined crack growth in three Ti-6Al-2Sn-4Zr-2Mo microstructures (globular α, elongated globular and colony) all of which showed surface and sub-surface cracks, and dwell fatigue crack growth was found to be faster in the non-colony structures. Pilchak et al [141] addressed non-dwell facet growth in Ti-6Al-4V with large colonies and observed facets growing along basal planes, finding that many thousands of cycles can contribute to the creation of a facet inclined close to 45° to the loading axis. Crack growth occurred over differently orientated α lamellae if the colonies shared a common basal plane orientation. Subsequent work [142] addressing non-dwell fatigue in fully lamellar Ti-6Al-4V found facets to be parallel, or near-parallel, to basal planes. FIB, EBSD and tilt fractography were employed to show that all cracks were found to nucleate at colony boundaries which were favourably orientated for slip transfer from $(0001)\langle 11\bar{2}0\rangle$ to $\{10\bar{1}1\}\langle 11\bar{2}\bar{3}\rangle$ systems in the adjacent grain. Fatigue lives for initiation resulting from the softer $<a_1>$ slip were significantly shorter than that initiated by $<a_2>$ slip. Later work by Pilchak [143] compared the growth rates associated with striation and facet growth mechanisms and found that faceted growth during dwell fatigue led to rates at least one to two orders of magnitude faster than that for striation growth.

To investigate strain development and crack nucleation in Ti-6Al-4V under both standard fatigue and dwell conditions Littlewood and Wilkinson [118, 144] utilized digital image correlation and high-resolution EBSD. Grain to grain interactions were found to be the primary cause of strain concentration and grains with <c>-axes near parallel to the macro-level loading showed very low strain levels with neighbouring grains having exceptionally high strain. The sites of high strain

concentration were found to coincide with the sites of crack nucleation both in fatigue and dwell fatigue.

7. Summary and discussion of future prospects and opportunities

Micromechanical deformation in HCP alloys involves a combination of effects that control component properties, such as cold dwell susceptibility. This starts from the rôle of different dislocation types and local atomic structure, such as micro-alloying, interstitial content and SRO on dislocation activity. The advent of new experimental approaches and improved simulation tools, such a strain gradient plasticity and fast simulation routes, will enable polycrystalline and single crystal methods to converge and utilise the same, physically motived, plasticity laws and constants rather than crude fitting to phenomenological hardening laws such as the Voce scheme and self-consistent approaches. The rôle of local interfaces and the precise chemistry of different phases in multi-component HCP alloys is an exciting prospect for further study and may enable us to engineer new alloys using novel chemistries and thermo-mechanical processing routes. Alleviation through processing and alloy design is often preferred by companies, as this reduces the financial burden in examples such as cold dwell fatigue. However, mechanistic understanding can also be used to guide service inspection programmes and operating environments once an alloy is put into service.

Rate and temperature sensitivity clearly plays a significant rôle in the evolution of microstructure during processing and the performance of alloys in high rate service deformation, such as bird strike. Here understanding the competition between different deformation modes at different temperatures and strain rates is required to qualify their behaviour and to design ideal operating modes for components in service. In particular the precise mechanisms behind deformation twinning are still not well understood, especially the rate determining steps and generation of suitable heterogeneities required for twin nucleation during the incubation period.

At longer time scales, such as in dwell fatigue, creep and stress relaxation play significant rôles in rate sensitive deformation modes. Mills and colleagues [69, 70, 95-99, 105, 122, 135] have provided an excellent basis for understanding creep and stress relaxation in titanium alloys. However, it would be informative to establish whether basal and prismatic slip are equally rate sensitive (similar to differing CRSS values) and give rise to the same relaxations of stress. Furthermore, this needs to be extended towards higher rate deformation and lower temperatures and to include the effects of micro-alloying, including the effect of interstitials and hydrogen, as compared to different β phase stabilisers in the Ti-6Al-2Sn-4Zr-XMo, where 2Mo shows the dwell debit and 6Mo does not [145]. It is not clear if this is a chemistry effect on dislocation motion and slip from α to β within the colony structure, or simply an effect of morphology, as different Mo content changes the structure slightly.

New complementary experimental and computational tools are quite promising to enable high quality models to be validated in exquisite detail, as well as exploration of new hypotheses prior to designing experimental tests. One particular area of interest is the rôle of the micro-texture, such as regions of common orientation, and the associated ‘rogue grain’ combination, that may be relevant to dwell debit. Experiments in this domain are challenging, as the statistics involved in finding an appropriate weakest link combined with enough cycles to demonstrate component-like failure modes is tricky at best. In particular, experimental quantification of the load shedding during stress or strain holds at the grain level is potentially crucial for the understanding of cold dwell fatigue, local load shedding and the generation of microstructure-level residual stress.

One exciting new avenue of study in this area is the potential combination of single crystal properties together with the precise mechanisms of slip transfer, such as work by Shirokoff et al [146], combined with local boundary strengths measured with HR-EBSD by Britton and Wilkinson [106] and Guo et al [107]. It is highly likely that the inhibition of slip and the resulting stress concentration at such interfaces play a key rôle in defect nucleation, and hence a systematic understanding of the rôle of the interface, the crystallographic orientation combination – such as the Burger orientation relationship in the context of α-β boundaries – are of great importance. This pushes the modelling community to develop new modelling strategies, where the discrete nature of plasticity within large numbers of grains must be captured; this will likely involve developing appropriate discrete dislocation plasticity models for slip transfer and inhibition and using these to inform higher-level modelling techniques such as crystal plasticity.

These prospects provide a rich and exciting space in which we can explore in tandem with experiments and simulations to develop new theories and mechanistic understanding. Our review highlights the complex rôles of chemistry and microstructure on micromechanical performance. In these highly engineered alloy systems, where alloy chemistries and thermo-mechanical processing are very tightly controlled, we have the prospect to tailor new alloys and microstructures to drive forward engineering of new components. To enhance introduction of these exciting alloys we must enhance our understanding of the micromechanical performance across chemistries, temperatures, microstructures and time scales. This will enable us to develop appropriate predictive modelling capability, rooted with high quality experimental evidence, to enable materials engineers to capitalize on the rich and diverse range of HCP alloys systems and deliver safe, secure and affordable technology for all.

8. Acknowledgements

We also thank Dr Terry Jun for generating a clear figure of the BOR seen in

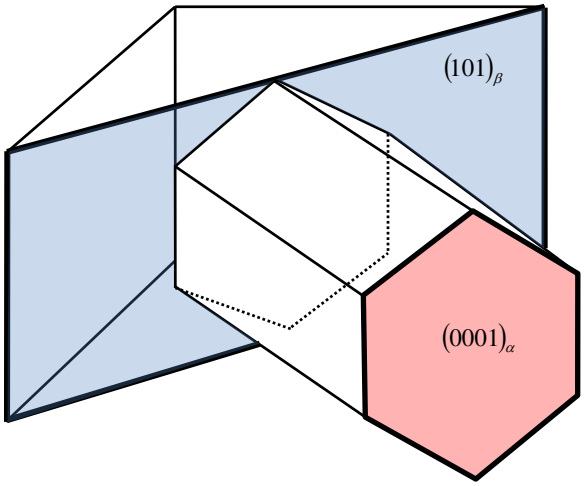

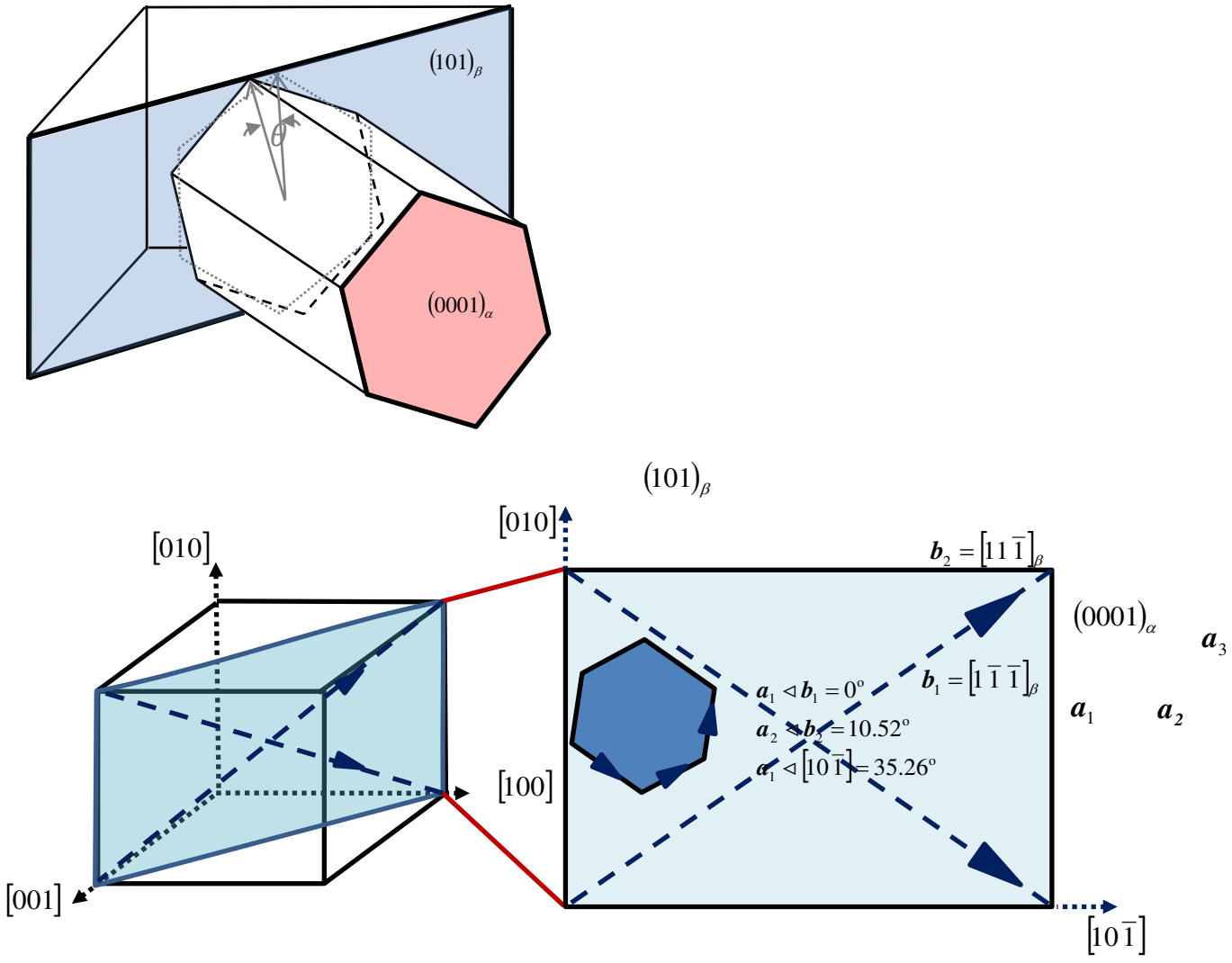

Figure 8.

9. Data accessibility statement

This is a review of existing literature and all data is referenced within the manuscript.

10. Competing interests statement

The authors declare no competing interests.

11. Authors' contributions statement

All three authors planned the manuscript, co-contributed to all significant sections and reviewed the entire manuscript in its complete form.

12. Funding statement

The authors acknowledge funding from the EPSRC for the HexMat Programme Grant (EP/K034332/1, for more information see http://www.imperial.ac.uk/hexmat).

13. References

1. Akhtar, A., *BASAL SLIP IN ZIRCONIUM.* Acta Metallurgica, 1973. **21**(1): p. 1-11.

2. Akhtar, A., *BASAL SLIP AND TWINNING IN ALPHA-TITANIUM SINGLE-CRYSTALS.* Metallurgical Transactions, 1975. **A 6**(5): p. 1105-1113.
3. Akhtar, A., *PRISMATIC SLIP IN ZIRCONIUM SINGLE-CRYSTALS AT ELEVATED-TEMPERATURES.* Metallurgical Transactions a-Physical Metallurgy and Materials Science, 1975. **6**(6): p. 1217-1222.
4. Akhtar, A. and Teghtsoo.A, *PLASTIC DEFORMATION OF ZIRCONIUM SINGLE CRYSTALS.* Acta Metallurgica, 1971. **19**(7): p. 655-&.
5. Turner, P.A. and C.N. Tome, *A STUDY OF RESIDUAL-STRESSES IN ZIRCALOY-2 WITH ROD TEXTURE.* Acta Metallurgica Et Materialia, 1994. **42**(12): p. 4143-4153.
6. Lebensohn, R.A. and C.N. Tome, *A SELF-CONSISTENT ANISOTROPIC APPROACH FOR THE SIMULATION OF PLASTIC-DEFORMATION AND TEXTURE DEVELOPMENT OF POLYCRYSTALS - APPLICATION TO ZIRCONIUM ALLOYS.* Acta Metallurgica Et Materialia, 1993. **41**(9): p. 2611-2624.
7. Eshelby, J.D., *THE DETERMINATION OF THE ELASTIC FIELD OF AN ELLIPSOIDAL INCLUSION, AND RELATED PROBLEMS.* Proceedings of the Royal Society of London Series a-Mathematical and Physical Sciences, 1957. **241**(1226): p. 376-396.
8. Eshelby, J.D., *THE ELASTIC FIELD OUTSIDE AN ELLIPSOIDAL INCLUSION.* Proceedings of the Royal Society of London Series a-Mathematical and Physical Sciences, 1959. **252**(1271): p. 561-569.
9. Hartley, C.S., et al., *A Comparison of Deformation Textures and Mechanical Properties Predicted by Different Crystal Plasticity Codes.* Materials Processing and Texture, 2009. **200**: p. 701-712.
10. Liu, B., et al., *Comparison of finite element and fast Fourier transform crystal plasticity solvers for texture prediction.* Modelling and Simulation in Materials Science and Engineering, 2010. **18**(8).
11. Rollett, A.D., S. Lee, and R.A. Lebensohn, *3D Image-Based Viscoplastic Response with Crystal Plasticity.* Microstructure and Texture in Steels and Other Materials, 2009: p. 255-264.
12. Merson, E., R. Brydson, and A. Brown, *The effect of crystallographic orientation on the mechanical properties of titanium*, in *Emag: Electron Microscopy and Analysis Group Conference 2007*, R.T. Baker, G. Mobus, and P.D. Brown, Editors. 2008.
13. Viswanathan, G.B., et al., *Direct observations and analyses alpha phase of an alpha/beta Ti-alloy of dislocation substructures in the formed by nanoindentation.* Acta Materialia, 2005. **53**(19): p. 5101-5115.
14. Britton, T.B., et al., *The effect of crystal orientation on the indentation response of commercially pure titanium: experiments and simulations.* Proceedings of the Royal Society a-Mathematical Physical and Engineering Sciences, 2010. **466**(2115): p. 695-719.
15. Zambaldi, C., et al., *Orientation informed nanoindentation of alpha-titanium: Indentation pileup in hexagonal metals deforming by prismatic slip.* Journal of Materials Research, 2012. **27**(1): p. 356-367.

16. Dimiduk, D.M., M.D. Uchic, and T.A. Parthasarathy, *Size-affected single-slip behavior of pure nickel microcrystals.* Acta Materialia, 2005. **53**(15): p. 4065-4077.
17. Gong, J.C. and A. Wilkinson, *Investigation of elastic properties of single-crystal alpha-Ti using microcantilever beams.* Philosophical Magazine Letters, 2010. **90**(7): p. 503-512.
18. Gong, J.C. and A.J. Wilkinson, *Anisotropy in the plastic flow properties of single-crystal alpha titanium determined from micro-cantilever beams.* Acta Materialia, 2009. **57**(19): p. 5693-5705.
19. Gong, J.C. and A.J. Wilkinson, *A microcantilever investigation of size effect, solid-solution strengthening and second-phase strengthening for < a > prism slip in alpha-Ti.* Acta Materialia, 2011. **59**(15): p. 5970-5981.
20. Gong, J.C. and A.J. Wilkinson, *Micro-cantilever testing of < a > prismatic slip in commercially pure Ti.* Philosophical Magazine, 2011. **91**(7-9): p. 1137-1149.
21. Ding, R.G., et al., *Transmission electron microscopy of deformed Ti-6Al-4V micro-cantilevers.* Philosophical Magazine, 2012. **92**(25-27): p. 3290-3314.
22. Ding, R.G., et al., *<c+a> deformation in Ti-6Al-4V micro-cantilevers.* Acta Materialia, 2014. **in press**.
23. Tarleton, E., et al., *A discrete dislocation plasticity study of the micro-cantilever size effect.* Acta Materialia, 2015. **88**: p. 271-282.
24. Byer, C.M. and K.T. Ramesh, *Effects of the initial dislocation density on size effects in single-crystal magnesium.* Acta Materialia, 2013. **61**(10): p. 3808-3818.
25. Lilleodden, E., *Microcompression study of Mg (0001) single crystal.* Scripta Materialia, 2010. **62**(8): p. 532-535.
26. Prasad, K.E., K. Rajesh, and U. Ramamurty, *Micropillar and macropillar compression responses of magnesium single crystals oriented for single slip or extension twinning.* Acta Materialia, 2014. **65**: p. 316-325.
27. Ye, J., et al., *In situ TEM compression testing of Mg and Mg-0.2 wt.% Ce single crystals.* Scripta Materialia, 2011. **64**(3): p. 292-295.
28. Sun, Q.Y., et al., *Size effects in strength and plasticity of single-crystalline titanium micropillars with prismatic slip orientation.* Scripta Materialia, 2011. **65**(6): p. 473-476.
29. Yu, Q., et al., *Strong crystal size effect on deformation twinning.* Nature, 2010. **463**(7279): p. 335-338.
30. Dunstan, D.J. and A.J. Bushby, *The scaling exponent in the size effect of small scale plastic deformation.* International Journal of Plasticity, 2013. **40**: p. 152-162.
31. Roscoe, R., *The plastic deformation of cadmium single-crystals.* Philosophical Magazine, 1936. **7**(21): p. 399-406.
32. Jillson, D.C., *QUANTITATIVE STRESS-STRAIN STUDIES ON ZINC SINGLE CRYSTALS IN TENSION.* Transactions of the American Institute of Mining and Metallurgical Engineers, 1950. **188**(9): p. 1129-1133.

33. Burke, E.C. and W.R. Hibbard, *PLASTIC DEFORMATION OF MAGNESIUM SINGLE CRYSTALS.* Transactions of the American Institute of Mining and Metallurgical Engineers, 1952. **194**(3): p. 295-303.
34. Jeffery, R.A. and E. Smith, *WORK-HARDENING AND DUCTILITY OF RHENIUM AND THEIR RELATION TO THE BEHAVIOURS OF OTHER METALS HAVING A HEXAGONAL STRUCTURE.* Nature, 1960. **187**(4731): p. 52-53.
35. Rapperport, E.J., *Room temperature deformation processes in zirconium*

Acta Metallurgica, 1959. **7**(4): p. 254-260.
36. Levine, E.D., *DEFORMATION MECHANISMS IN TITANIUM AT LOW TEMPERATURES.* Transactions of the Metallurgical Society of Aime, 1966. **236**(11): p. 1558-&.
37. Snow, D.B. and J.F. Breedis, *Deformation of single-crystal ruthenium.* Acta Metallurgica, 1974. **22**(4): p. 419-427.
38. Das, G. and T.E. Mitchell, *MECHANICAL PROPERTIES OF HAFNIUM SINGLE-CRYSTALS.* Metallurgical Transactions, 1973. **4**(5): p. 1405-1413.
39. Turner, G.I. and J.S. White, *TEMPERATURE DEPENDENCE OF CRITICAL RESOLVED SHEAR STRESSES FOR BASAL AND PRISMATIC SLIP IN BERYLLIUM.* Scripta Metallurgica, 1972. **6**(2): p. 123-&.
40. Bacon, D.J. and V. Vitek, *Atomic-scale modeling of dislocations and related properties in the hexagonal-close-packed metals.* Metallurgical and Materials Transactions a-Physical Metallurgy and Materials Science, 2002. **33**(3): p. 721-733.
41. Girshick, A., D.G. Pettifor, and V. Vitek, *Atomistic simulation of titanium - II. Structure of 1/3 <(1)over-bar2(1)over-bar0 > screw dislocations and slip systems in titanium.* Philosophical Magazine a-Physics of Condensed Matter Structure Defects and Mechanical Properties, 1998. **77**(4): p. 999-1012.
42. Ghazisaeidi, M. and D.R. Trinkle, *Core structure of a screw dislocation in Ti from density functional theory and classical potentials.* Acta Materialia, 2012. **60**(3): p. 1287-1292.
43. Tarrat, N., et al., *Screw dislocation in hcp Ti : DFT dislocation excess energies and metastable core structures.* Modelling and Simulation in Materials Science and Engineering, 2014. **22**(5).
44. Adhikari, S. and P. Mukhopadhyay, *Physical Metallurgy of Beryllium and Its Alloys.* Mineral Processing and Extractive Metallurgy Review, 1995. **14**(1): p. 253-299.
45. Soo, P. and G.T. Higgins, *DEFORMATION OF ZIRCONIUM-OXYGEN SINGLE CRYSTALS.* Acta Metallurgica, 1968. **16**(2): p. 177-&.
46. Paton, N.E. and W.A. Backofen, *Plastic deformation of titanium at elevated temperatures.* Metallurgical Transactions, 1970. **1**(10): p. 2839-&.
47. Tanaka, T. and H. Conrad, *DEFORMATION KINETICS FOR (1010)(1120) SLIP IN TITANIUM SINGLE-CRYSTALS BELOW 0.4TM.* Acta Metallurgica, 1972. **20**(8): p. 1019-&.
48. Akhtar, A. and E. Teghtsoonian, *PRISMATIC SLIP IN ALPHA-TITANIUM SINGLE-CRYSTALS.* Metallurgical Transactions a-Physical Metallurgy and Materials Science, 1975. **6**(12): p. 2201-2208.

49. Sheely, W.F. and R.R. Nash, *MECHANICAL PROPERTIES OF MAGNESIUM MONOCRYSTALS.* Transactions of the American Institute of Mining and Metallurgical Engineers, 1960. **218**(3): p. 416-423.
50. Conrad, H., *EFFECT OF INTERSTITIAL SOLUTES ON THE STRENGTH AND DUCTILITY OF TITANIUM.* Progress in Materials Science, 1981. **26**(2-4): p. 123-404.
51. Williams, J.C. and M.J. Blackburn, *The identification of a Non-Basal slip vector in titanium and titanium-aluminium alloys.* Physica Status Solidi (b), 1968. **25**(1): p. K1-K3.
52. Akhtar, A., *Compression of Zirconium Single-Crystals Parallel to C-Axis.* Journal of Nuclear Materials, 1973. **47**(1): p. 79-86.
53. Williams, J.C., R.G. Baggerly, and N.E. Paton, *Deformation behavior of HCPTi-Al alloy single crystals.* Metallurgical and Materials Transactions a-Physical Metallurgy and Materials Science, 2002. **33**(3): p. 837-850.
54. Monnet, G., B. Devincre, and L.P. Kubin, *Dislocation study of prismatic slip systems and their interactions in hexagonal close packed metals: application to zirconium.* Acta Materialia, 2004. **52**(14): p. 4317-4328.
55. Monnet, G., L. Vincent, and B. Devincre, *Dislocation-dynamics based crystal plasticity law for the low- and high-temperature deformation regimes of bcc crystal.* Acta Materialia, 2013. **61**(16): p. 6178-6190.
56. Churchman, A.T., *THE SLIP MODES OF TITANIUM AND THE EFFECT OF PURITY ON THEIR OCCURRENCE DURING TENSILE DEFORMATION OF SINGLE CRYSTALS.* Proceedings of the Royal Society of London Series a-Mathematical and Physical Sciences, 1954. **226**(1165): p. 216-226.
57. Lutjering, G. and J.C. Williams, *Titanium*. 2007: Springer Science and Business Media.
58. Yu, Q., et al., *Origin of dramatic oxygen solute strengthening effect in titanium.* Science, 2015. **347**(6222): p. 635-639.
59. Williams, J.C., P.P. Tung, and A.W. Sommer, *INFLUENCE OF OXYGEN CONCENTRATION ON INTERNAL STRESS AND DISLOCATION ARRANGEMENTS IN ALPHA TITANIUM.* Metallurgical Transactions, 1972. **3**(11): p. 2979-&.
60. Welsch, G. and W. Bunk, *DEFORMATION MODES OF THE ALPHA-PHASE OF TI-6AL-4V AS A FUNCTION OF OXYGEN CONCENTRATION AND AGING TEMPERATURE.* Metallurgical Transactions a-Physical Metallurgy and Materials Science, 1982. **13**(5): p. 889-899.
61. Anderson, E.A., D.C. Jillson, and S.R. Dunbar, *DEFORMATION MECHANISMS IN ALPHA-TITANIUM.* Transactions of the American Institute of Mining and Metallurgical Engineers, 1953. **197**(9): p. 1191-1197.
62. Skippon, T., C. Mareau, and M.R. Daymond, *On the determination of single-crystal plasticity parameters by diffraction: optimization of a polycrystalline plasticity model using a genetic algorithm.* Journal of Applied Crystallography, 2012. **45**: p. 627-643.
63. Rugg, D., et al., *In-service materials support for safety critical applications - A case study of a high strength Ti-alloy using advanced experimental and*

modelling techniques. Materials Science and Engineering a-Structural Materials Properties Microstructure and Processing, 2014. **599**: p. 166-173.
64. Pilchak, A.L., W.J. Porter, and R. John, *Room temperature fracture processes of a near-alpha titanium alloy following elevated temperature exposure.* Journal of Materials Science, 2012. **47**(20): p. 7235-7253.
65. Parthasarathy, T.A., et al., *Life prediction under tension of titanium alloys that develop an oxygenated brittle case during use.* Scripta Materialia, 2011. **65**(5): p. 420-423.
66. Sakai, T. and M.E. Fine, *PLASTIC-DEFORMATION OF TI-AL SINGLE-CRYSTALS IN PRISMATIC SLIP.* Acta Metallurgica, 1974. **22**(11): p. 1359-1372.
67. Sakai, T. and M.E. Fine, *FAILURE OF SCHMIDS LAW IN TI-A1 ALLOYS FOR PRISMATIC SLIP.* Scripta Metallurgica, 1974. **8**(5): p. 541-544.
68. Sakai, T. and M.E. Fine, *BASAL SLIP OF TI-A1 SINGLE-CRYSTALS.* Scripta Metallurgica, 1974. **8**(5): p. 545-547.
69. Neeraj, T., et al., *Phenonomenological and microstructural analysis of room temperature creep in titanium alloys.* Acta Materialia, 2000. **48**(6): p. 1225-1238.
70. Neeraj, T. and M.J. Mills, *Short-range order (SRO) and its effect on the primary creep behavior of a Ti-6wt.%Al alloy.* Materials Science and Engineering a-Structural Materials Properties Microstructure and Processing, 2001. **319**: p. 415-419.
71. Christian, J.W. and S. Mahajan, *Deformation Twinning.* Progress in Materials Science, 1995. **39**: p. 1-157.
72. Yoo, M.H., *Slip, Twinning, and Fracture in Hexagonal Close-Packed Metals.* Metallurgical and Materials Transactions a-Physical Metallurgy and Materials Science, 1981. **12A**: p. 409.
73. Tenckhoff, E., *Review of deformation mechanisms, texture, and mechanical anisotropy in zirconium and zirconium base alloys.* Zirconium in the Nuclear Industry: 14th International Symposium, 2005. **1467**: p. 25-50.
74. Agnew, S.R., J.A. Horton, and M.H. Yoo, *Transmission electron microscopy investigation of < c+a > dislocations in Mg and alpha-solid solution Mg-Li alloys.* Metallurgical and Materials Transactions a-Physical Metallurgy and Materials Science, 2002. **33**(3): p. 851-858.
75. Yang, Y., et al., *Characterization and Modeling of Heterogeneous Deformation in Commercial Purity Titanium.* Jom, 2011. **63**(9): p. 66-73.
76. Bieler, T.R., et al., *Strain Heterogeneity and Damage Nucleation at Grain Boundaries during Monotonic Deformation in Commercial Purity Titanium.* Jom, 2009. **61**(12): p. 45-52.
77. Bieler, T.R., et al., *The role of heterogeneous deformation on damage nucleation at grain boundaries in single phase metals.* International Journal of Plasticity, 2009. **25**(9): p. 1655-1683.

78. Wang, L., et al., *Twin Nucleation by Slip Transfer across Grain Boundaries in Commercial Purity Titanium.* Metallurgical and Materials Transactions a-Physical Metallurgy and Materials Science, 2010. **41a**(2): p. 421-430.
79. Ghaderi, A. and M.R. Barnett, *Sensitivity of deformation twinning to grain size in titanium and magnesium.* Acta Materialia, 2011. **59**(20): p. 7824-7839.
80. Wang, J., et al., *Twinning dislocations on {(1)over-bar011} and {(1)over-bar013} planes in hexagonal close-packed crystals.* Acta Materialia, 2011. **59**(10): p. 3990-4001.
81. Wang, J., J.P. Hirth, and C.N. Tome, *((1)over-bar0 1 2) Twinning nucleation mechanisms in hexagonal-close-packed crystals.* Acta Materialia, 2009. **57**(18): p. 5521-5530.
82. Wang, J., et al., *Nucleation of a ((1)over-bar 0 1 2) twin in hexagonal close-packed crystals.* Scripta Materialia, 2009. **61**(9): p. 903-906.
83. Agnew, S.R., et al., *Study of slip mechanisms in a magnesium alloy by neutron diffraction and modeling.* Scripta Materialia, 2003. **48**(8): p. 1003-1008.
84. Lee, S.Y., et al., *Deformation behaviour of solid-solution-strengthened Mg-9 wt.% Al alloy: In situ neutron diffraction and elastic-viscoplastic self-consistent modeling.* Acta Materialia, 2014. **73**: p. 139-148.
85. Capolungo, L., et al., *Nucleation and growth of twins in Zr: A statistical study.* Acta Materialia, 2009. **57**(20): p. 6047-6056.
86. Prakash, D.G.L., et al., *Deformation twinning in Ti-6Al-4V during low strain rate deformation to moderate strains at room temperature.* Materials Science and Engineering a-Structural Materials Properties Microstructure and Processing, 2010. **527**(21-22): p. 5734-5744.
87. Beyerlein, I.J., et al., *Statistical analyses of deformation twinning in magnesium.* Philosophical Magazine, 2010. **90**(16): p. 2161-2190.
88. Beyerlein, I.J. and C.N. Tome, *A probabilistic twin nucleation model for HCP polycrystalline metals.* Proceedings of the Royal Society a-Mathematical Physical and Engineering Sciences, 2010. **466**(2121): p. 2517-2544.
89. Abdolvand, H. and M.R. Daymond, *Multi-scale modeling and experimental study of twin inception and propagation in hexagonal close-packed materials using a crystal plasticity finite element approach; part II: Local behavior.* Journal of the Mechanics and Physics of Solids, 2013. **61**(3): p. 803-818.
90. Abdolvand, H. and M.R. Daymond, *Multi-scale modeling and experimental study of twin inception and propagation in hexagonal close-packed materials using a crystal plasticity finite element approach-Part I: Average behavior.* Journal of the Mechanics and Physics of Solids, 2013. **61**(3): p. 783-802.
91. Wang, L.Y., et al., *Study of Twinning in alpha-Ti by EBSD and Laue Microdiffraction.* Metallurgical and Materials Transactions a-Physical Metallurgy and Materials Science, 2013. **44A**(8): p. 3664-3674.

92. Bieler, T.R., et al., *In Situ Characterization of Twin Nucleation in Pure Ti Using 3D-XRD.* Metallurgical and Materials Transactions a-Physical Metallurgy and Materials Science, 2014. **45A**(1): p. 109-122.
93. Aydiner, C.C., et al., *Evolution of stress in individual grains and twins in a magnesium alloy aggregate.* Physical Review B, 2009. **80**(2).
94. Lynch, P.A., et al., *Time and spatial resolution of slip and twinning in a grain embedded within a magnesium polycrystal.* Acta Materialia, 2014. **78**: p. 203-212.
95. Suri, S., et al., *Room temperature deformation and mechanisms of slip transmission in oriented single-colony crystals of an alpha/beta titanium alloy.* Acta Materialia, 1999. **47**(3): p. 1019-1034.
96. Neeraj, T., et al., *Observation of tension-compression asymmetry in alpha and alpha/beta titanium alloys.* Philosophical Magazine, 2005. **85**(2-3): p. 279-295.
97. Savage, M.F., J. Tatalovich, and M.J. Mills, *Anisotropy in the room-temperature deformation of alpha-beta colonies in titanium alloys: role of the alpha-beta interface.* Philosophical Magazine, 2004. **84**(11): p. 1127-1154.
98. Savage, M.F., et al., *Deformation mechanisms and microtensile behavior of single colony Ti-6242Si.* Materials Science and Engineering a-Structural Materials Properties Microstructure and Processing, 2001. **319**: p. 398-403.
99. Venkatramani, G., S. Ghosh, and M. Mills, *A size-dependent crystal plasticity finite-element model for creep and load shedding in polycrystalline titanium alloys.* Acta Materialia, 2007. **55**(11): p. 3971-3986.
100. Shi, R., et al., *Variant selection of grain boundary $\mathfrak{Co}$ by special prior $\mathfrak{Q}$ grain boundaries in titanium alloys.* Acta Materialia, 2014. **75**: p. 156-166.
101. Chan, K.S., C.C. Wojcik, and D.A. Koss, *Deformation of an alloy with a lamellar microstructure: experimental behavior of individual widmanstatten colonies of an α-β titanium alloy.* Metallurgical Transactions A, 1981. **12**(11): p. 1899-1907.
102. Ankem, S. and H. Margolin, Metallurgical and Materials Transactions a-Physical Metallurgy and Materials Science, 1983. **14A**: p. 500-503.
103. Ambard, A., et al., *Role of interphases in the deformation mechanisms of an alpha/beta titanium alloy at 20 K.* Materials Science and Engineering a-Structural Materials Properties Microstructure and Processing, 2001. **319**: p. 404-408.
104. Feaugas, X. and M. Clavel, *Cyclic deformation behaviour of an alpha/beta titanium alloy .1. Micromechanisms of plasticity under various loading paths.* Acta Materialia, 1997. **45**(7): p. 2685-2701.
105. Savage, M.F., T. Neeraj, and M.J. Mills, *Observations of room-temperature creep recovery in titanium alloys.* Metallurgical and Materials Transactions a-Physical Metallurgy and Materials Science, 2002. **33**(3): p. 891-898.

106. Britton, T.B. and A.J. Wilkinson, *Stress fields and geometrically necessary dislocation density distributions near the head of a blocked slip band.* Acta Materialia, 2012. **60**(16): p. 5773-5782.
107. Guo, Y., T.B. Britton, and A.J. Wilkinson, *Slip band-grain boundary interactions in commercial-purity titanium.* Acta Materialia, 2014. **76**: p. 1-12.
108. Medina Perilla, J.A. and J. Gil Sevillano, *Two-dimensional sections of the yield locus of a Ti・6%Al・4%V alloy with a strong transverse-type crystallographic α-texture.* Materials Science and Engineering A, 1995. **201**(1-2): p. 103-110.
109. Jones, I.P. and W.B. Hutchinson, *Stress-State Dependence of Slip in Titanium-6a1-4v and Other Hcp Metals.* Acta Metallurgica, 1981. **29**(6): p. 951-968.
110. Ding, R.G., et al., *< c plus a > Dislocations in deformed Ti-6A1-4V micro-cantilevers.* Acta Materialia, 2014. **76**: p. 127-134.
111. Zhang, M., J. Zhang, and D.L. McDowell, *Micro structure-based crystal plasticity modeling of cyclic deformation of Ti-6Al-4V.* International Journal of Plasticity, 2007. **23**(8): p. 1328-1348.
112. Mayeur, J.R. and D.L. McDowell, *A three-dimensional crystal plasticity model for duplex Ti-6Al-4V.* International Journal of Plasticity, 2007. **23**(9): p. 1457-1485.
113. Dunne, F.P.E., D. Rugg, and A. Walker, *Lengthscale-dependent, elastically anisotropic, physically-based hcp crystal plasticity: Application to cold-dwell fatigue in Ti alloys.* International Journal of Plasticity, 2007. **23**(6): p. 1061-1083.
114. Dunne, F.P.E., A. Walker, and D. Rugg, *A systematic study of hcp crystal orientation and morphology effects in polycrystal deformation and fatigue.* Proceedings of the Royal Society a-Mathematical Physical and Engineering Sciences, 2007. **463**(2082): p. 1467-1489.
115. Dunne, F.P.E., R. Kiwanuka, and A.J. Wilkinson, *Crystal plasticity analysis of micro-deformation, lattice rotation and geometrically necessary dislocation density.* Proceedings of the Royal Society a-Mathematical Physical and Engineering Sciences, 2012. **468**(2145): p. 2509-2531.
116. Britton, T.B., et al., *Electron backscatter diffraction study of dislocation content of a macrozone in hot-rolled Ti-6Al-4V alloy.* Scripta Materialia, 2010. **62**(9): p. 639-642.
117. Littlewood, P.D., T.B. Britton, and A.J. Wilkinson, *Geometrically necessary dislocation density distributions in Ti-6Al-4V deformed in tension.* Acta Materialia, 2011. **59**(16): p. 6489-6500.
118. Littlewood, P.D. and A.J. Wilkinson, *Geometrically necessary dislocation density distributions in cyclically deformed Ti-6Al-4V.* Acta Materialia, 2012. **60**(15): p. 5516-5525.
119. Warwick, J.L.W., et al., *Effect of texture on load partitioning in Ti-6Al-4V.* Acta Materialia, 2012. **60**(10): p. 4117-4127.

120. Warwick, J.L.W., et al., *Lattice strain evolution during tensile and compressive loading of CP Ti.* Acta Materialia, 2012. **60**(19): p. 6720-6731.
121. Harrison, W.J., M.T. Whittaker, and R.J. Lancaster, *A model for time dependent strain accumulation and damage at low temperatures in Ti-6Al-4V.* Materials Science and Engineering a-Structural Materials Properties Microstructure and Processing, 2013. **574**: p. 130-136.
122. Hasija, V., et al., *Deformation and creep modeling in polycrystalline Ti-6Al alloys.* Acta Materialia, 2003. **51**(15): p. 4533-4549.
123. Rugg, D., M. Dixon, and F.P.E. Dunne, *Effective structural unit size in titanium alloys.* Journal of Strain Analysis for Engineering Design, 2007. **42**(4): p. 269-279.
124. Rugg, D. 2014.
125. Bache, M.R., *A review of dwell sensitive fatigue in titanium alloys: the role of microstructure, texture and operating conditions.* International Journal of Fatigue, 2003. **25**(9-11): p. 1079-1087.
126. Stroh, A.N., Proceedings of the Royal Society a-Mathematical Physical and Engineering Sciences, 1954. **223**: p. 404-414.
127. Lefranc, P., et al., *Nucleation of cracks from shear-induced cavities in an alpha/beta titanium alloy in fatigue, room-temperature creep and dwell-fatigue.* Acta Materialia, 2008. **56**(16): p. 4450-4457.
128. Gerland, M., et al., *Deformation and damage mechanisms in an alpha/beta 6242 Ti alloy in fatigue, dwell-fatigue and creep at room temperature. Influence of internal hydrogen.* Materials Science and Engineering a-Structural Materials Properties Microstructure and Processing, 2009. **507**(1-2): p. 132-143.
129. Bridier, F., P. Villechaise, and J. Mendez, *Slip and fatigue crack formation processes in an alpha/beta titanium alloy in relation to crystallographic texture on different scales.* Acta Materialia, 2008. **56**(15): p. 3951-3962.
130. Germain, L., et al., *Analysis of sharp microtexture heterogeneities in a bimodal IMI 834 billet.* Acta Materialia, 2005. **53**(13): p. 3535-3543.
131. Germain, L., et al., *Texture heterogeneities induced by subtransus processing of near alpha titanium alloys.* Acta Materialia, 2008. **56**(16): p. 4298-4308.
132. Uta, E., et al., *Texture heterogeneities in alpha(p)/alpha(s) titanium forging analysed by EBSD-Relation to fatigue crack propagation.* Journal of Microscopy, 2009. **233**(3): p. 451-459.
133. Dunne, F.P.E. and D. Rugg, *On the mechanisms of fatigue facet nucleation in titanium alloys.* Fatigue & Fracture of Engineering Materials & Structures, 2008. **31**(11): p. 949-958.
134. Bache, M.R., F.P.E. Dunne, and C. Madrigal, *Experimental and crystal plasticity studies of deformation and crack nucleation in a titanium alloy.* Journal of Strain Analysis for Engineering Design, 2010. **45**(5): p. 391-399.
135. Sinha, V., et al., *Observations on the faceted initiation site in the dwell-fatigue tested Ti-6242 alloy: Crystallographic orientation and size effects.* Metallurgical and Materials Transactions a-Physical Metallurgy and Materials Science, 2006. **37A**(5): p. 1507-1518.

136. Kirane, K. and S. Ghosh, *A cold dwell fatigue crack nucleation criterion for polycrystalline Ti-6242 using grain-level crystal plasticity FE Model.* International Journal of Fatigue, 2008. **30**(12): p. 2127-2139.
137. Anahid, M., M.K. Samal, and S. Ghosh, *Dwell fatigue crack nucleation model based on crystal plasticity finite element simulations of polycrystalline titanium alloys.* Journal of the Mechanics and Physics of Solids, 2011. **59**(10): p. 2157-2176.
138. Pilchak, A.L. and J.C. Williams, *Observations of Facet Formation in Near-alpha Titanium and Comments on the Role of Hydrogen.* Metallurgical and Materials Transactions a-Physical Metallurgy and Materials Science, 2011. **42A**(4): p. 1000-1027.
139. Pilchak, A.L., *A simple model to account for the role of microtexture on fatigue and dwell fatigue lifetimes of titanium alloys.* Scripta Materialia, 2014. **74**: p. 68-71.
140. McBagonluri, F., et al., *An investigation of the effects of microstructure on dwell fatigue crack growth in Ti-6242.* Materials Science and Engineering a-Structural Materials Properties Microstructure and Processing, 2005. **405**(1-2): p. 111-134.
141. Pilchak, A.L., et al., *Low Delta K faceted crack growth in titanium alloys.* International Journal of Fatigue, 2009. **31**(5): p. 989-994.
142. Pilchak, A.L., R.E.A. Williams, and J.C. Williams, Metallurgical and Materials Transactions a-Physical Metallurgy and Materials Science, 2010. **41A**: p. 106-124.
143. Pilchak, A.L., *Fatigue crack growth rates in alpha titanium: Faceted vs. striation growth.* Scripta Materialia, 2013. **68**(5): p. 277-280.
144. Littlewood, P.D. and A.J. Wilkinson, *Local deformation patterns in Ti-6Al-4V under tensile, fatigue and dwell fatigue loading.* International Journal of Fatigue, 2012. **43**: p. 111-119.
145. Qui, J., et al., Metallurgical and Materials Transactions a-Physical Metallurgy and Materials Science, 2014. **45A**: p. 6075-6087.
146. Shirokoff, J., I.M. Robertson, and H.K. Birnbaum, *The Slip Transfer Process through Grain-Boundaries in Hcp Ti.* Defect-Interface Interactions, 1994. **319**: p. 263-272.

List of figures:

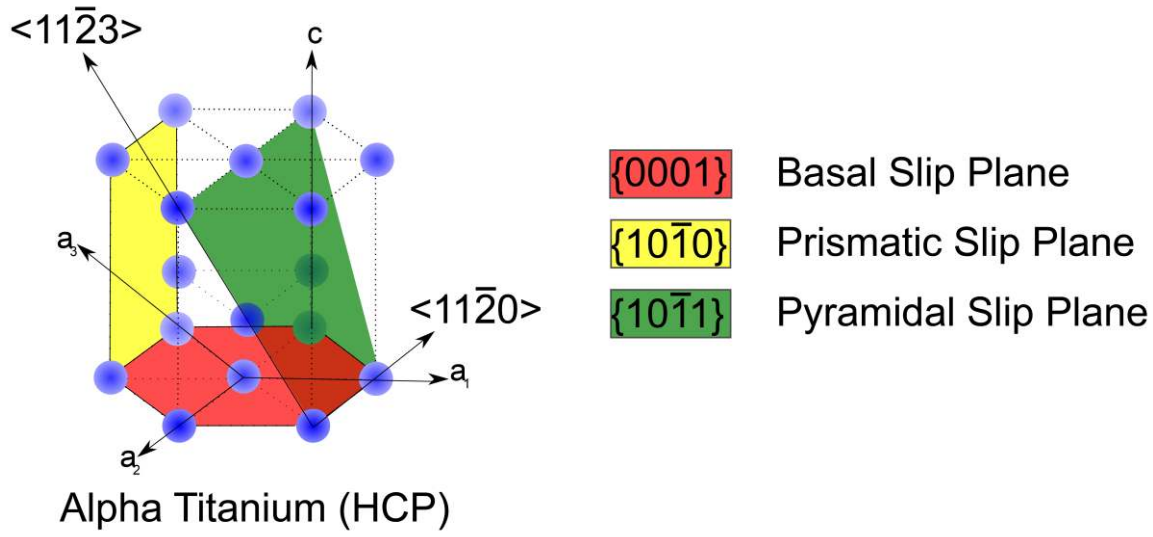

Figure 1: Slip systems in HCP metals and alloys.

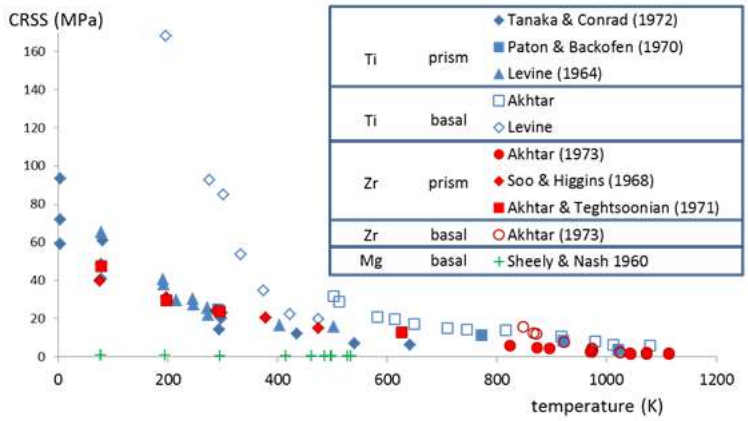

Figure 2: CRSS values for basal and prism slip in Ti [2, 36, 46, 47], Zr [1, 3, 4, 45] and Mg [49] single crystals with very low interstitial content.

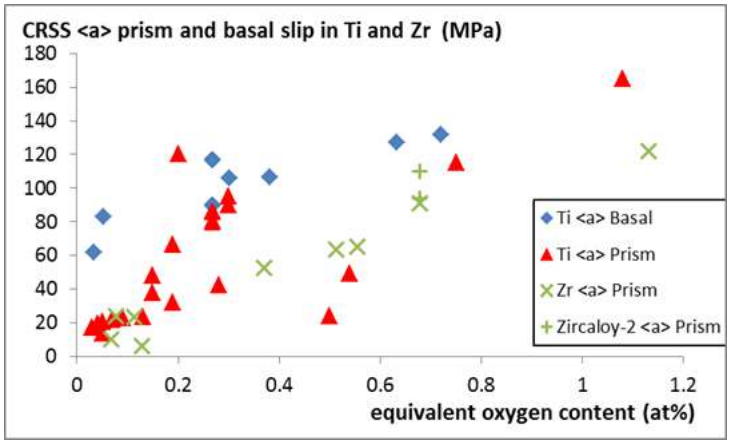

Figure 3: Effect of interstitial content on CRSS of Ti [18, 36, 50, 56, 61] and Zr [4, 5, 35, 45, 62] at room temperature.

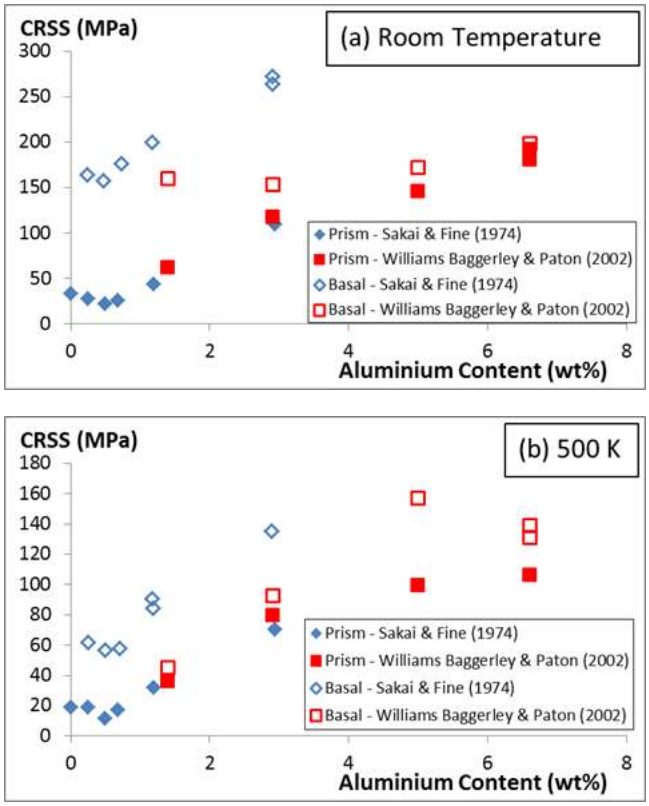

Figure 4: Effect of Al addition on CRSS values for prism slip and basal slip in Ti at (a) room temperature and (b) 500 K. [53, 66, 68]

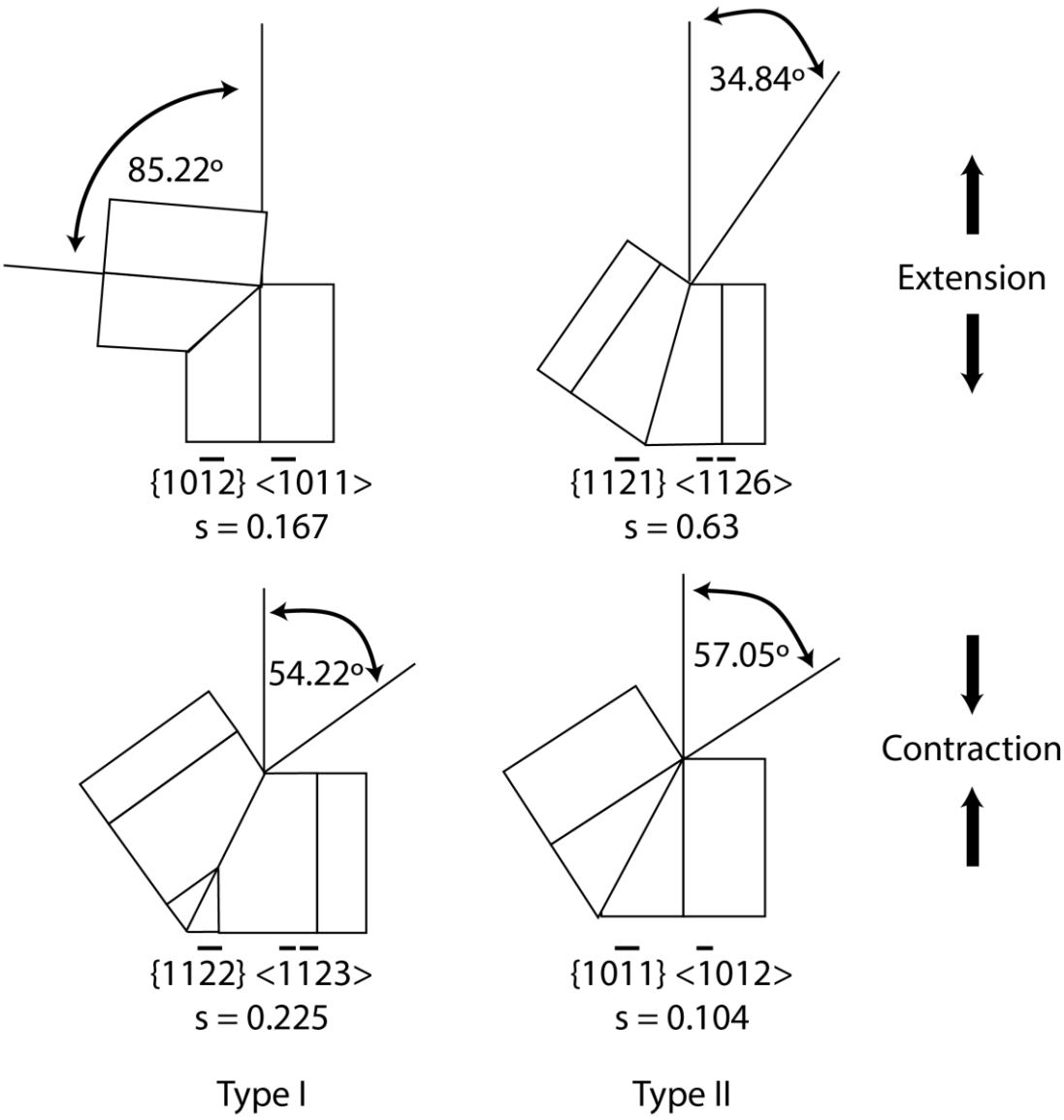

Figure 5: Twin systems in HCP-Zr (after Tenckhoff [73]).

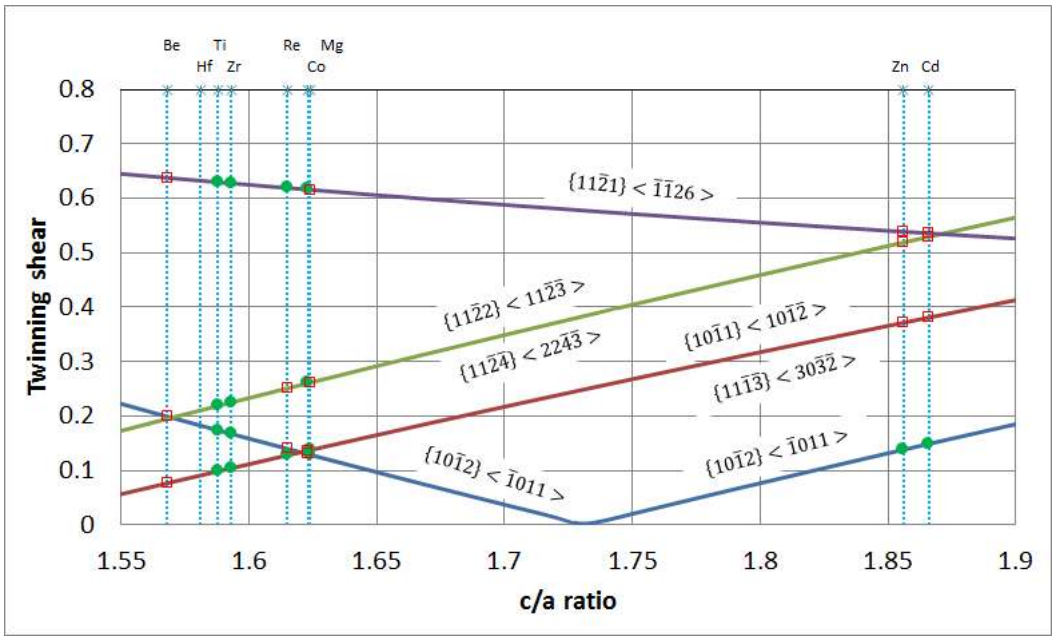

Figure 6: Twinning shear a function of c/a ratio in HCP crystals; filled green circles denote readily active twinning modes and red empty squares denote less active twinning modes (after Yoo [72]). Labelling of each twin system indicates the K_1 and K_2 twinning planes and the η_1 and η_2 invariant twin directions. Note the inversion of the $\{10\bar{1}2\} < \bar{1}011 >$ mode which indicates its change from an extension twin for low c/a materials to a contraction twin for high c/a materials.

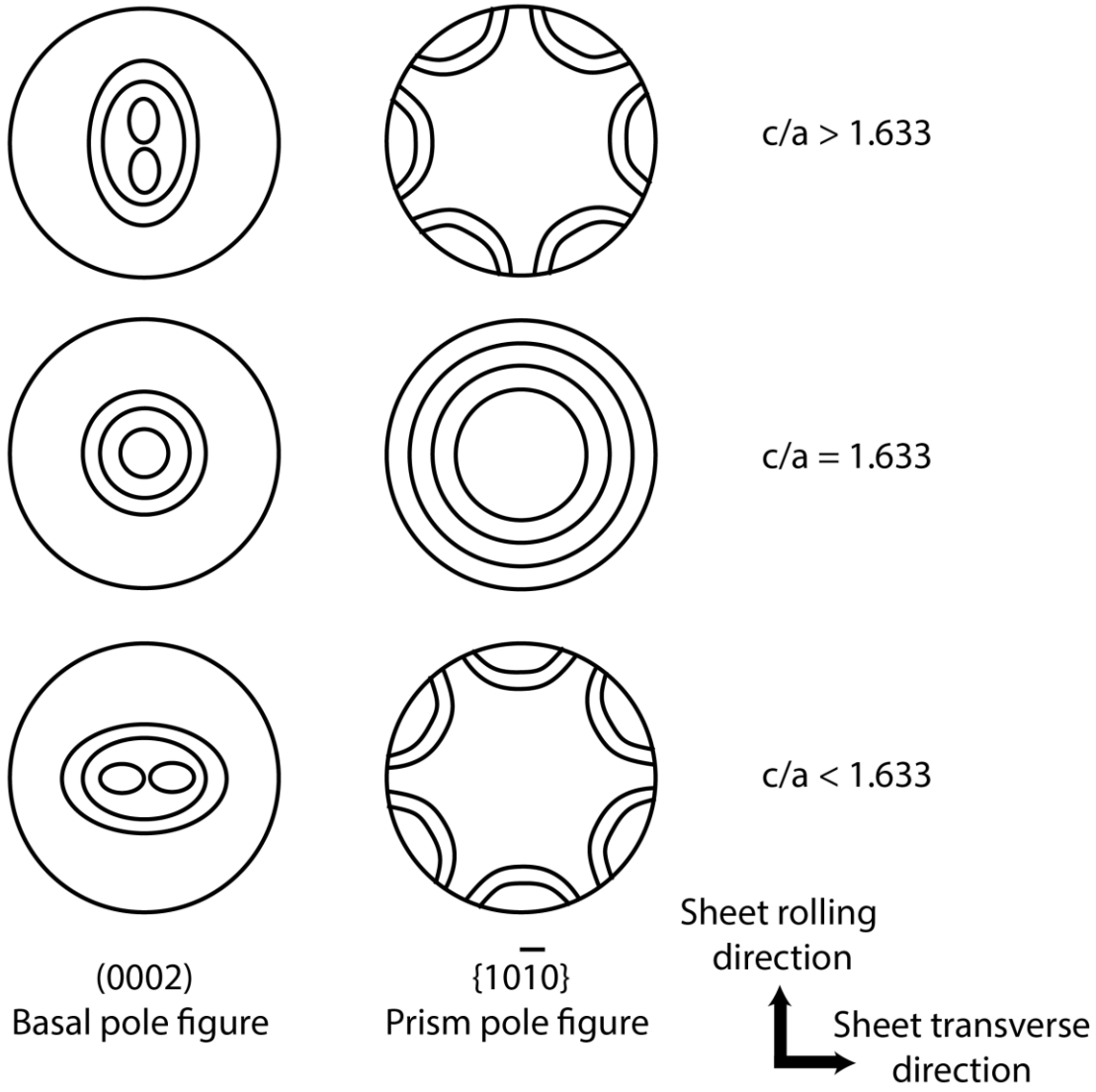

Figure 7: Example sheet textures for different c/a ratios associated with twinning (after Tenckhoff [73]).

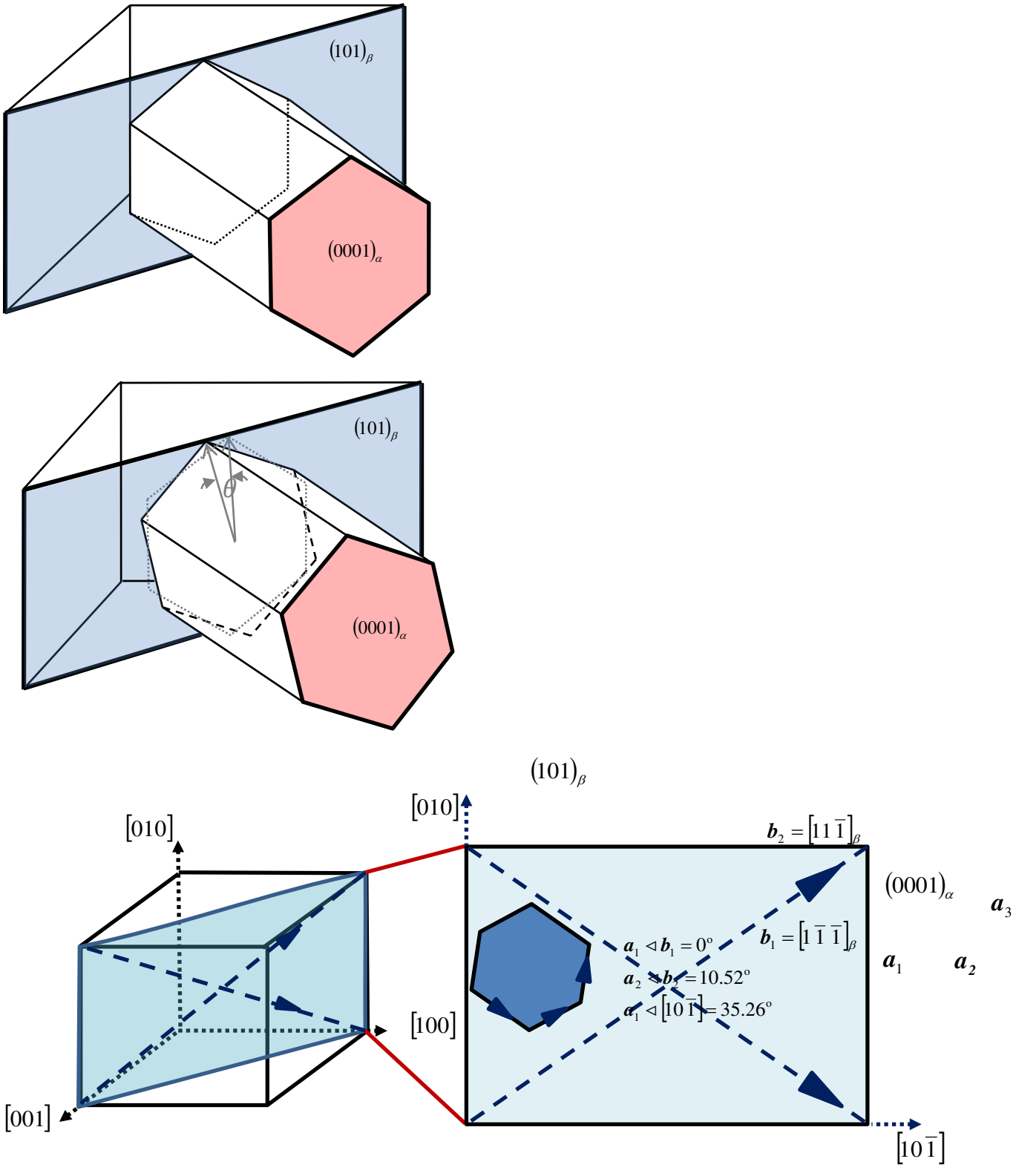

Figure 8: Diagram showing (a) schematic of an alpha (hcp) – beta (bcc) interface, (b) the quantitative Burger Orientation Relationship (BOR) which exists for a coherent interface between adjacent HCP α and BCC β laths, and (c) a schematic showing an incoherent interface between HCP α and BCC β laths.

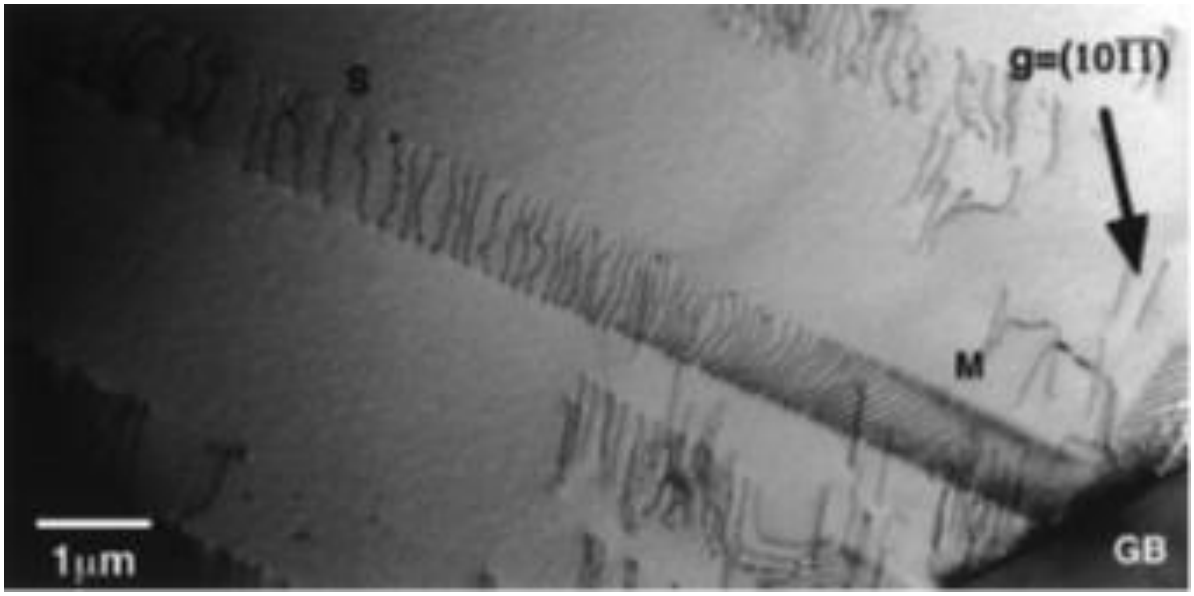

Figure 9: A slip band (comprising mostly <a> type slip) developed in creep impinging on a grain boundary, with dislocations of mixed mode (M) close to the grain boundary and screw (S) within the bulk of the α grain [105].